Building and Environment

Boundary Layer Wind Tunnel Modeling Experiments on Pumping Ventilation through a Three-Story Reduce-Scaled Building with Two Openings

--Manuscript Draft--

Manuscript Number:	BAE-D-21-00155R2
Article Type:	VSI: Urban Morphology
Keywords:	Pumping ventilation; Single-sided ventilation; Vortex shedding; wind tunnel experiments; Natural ventilation.
Corresponding Author:	Fu-Yun Zhao, Ph.D Wuhan University Wuhan, CHINA
First Author:	Huai-Yu Zhong, Ph.D
Order of Authors:	Huai-Yu Zhong, Ph.D
	Chao Lin, Ph.D
	Yang Sun, Ph.D
	Hideki Kikumoto, Ph.D
	Ryozo Ooka, Ph.D
	Hong-Liang Zhang, Ph.D
	Hong Hu, Ph.D
	Fu-Yun Zhao, Ph.D
	Carlos Jimenez-Bescos, Ph.D
Abstract:	Pumping ventilation is a special single-sided wind driven building ventilation induced by periodic vortex shedding at the building wake. This work aimed to investigate the oscillating frequency at the building façade opening and ventilation rate of pumping ventilation. The effects of opening separations on different floors of a three-story reduce-scaled building with two openings were considered using boundary-layer wind tunnel experiments. The wind velocity of the surrounding flow field and the center of the opening were measured. The ventilation rate was obtained by tracer gas method with constant and continuous injection rate. The results showed that the oscillating frequency was independent of the opening separation except on the third floor probably because of the disturbance of the rooftop shedding frequency. The oscillating frequency on the first floor was the lowest due to the resistance of the ground to the vortex shedding. Pumping ventilation indicated that its ventilation rate is greater than that of general ventilation across the single opening with the same total opening area. The promotion of ventilation rate was up to about 123% on the first floor, about 65% on the second floor and about 44% on the third floor. Expansion of opening separations could boost the ventilation rate. Meanwhile, the fluctuation of opening center wind velocity and indoor species concentration were not positively correlated with the ventilation rate of pumping ventilation. Conclusions of this research could provide some useful reference to the design of natural ventilation for buildings.

Abstract and keywords

Abstract

Pumping ventilation is a special single-sided wind driven building ventilation induced by periodic vortex shedding at the building wake. This work aimed to investigate the oscillating frequency at the building façade opening and ventilation rate of pumping ventilation. The effects of opening separations on different floors of a three-story reduce-scaled building with two openings were considered using boundary-layer wind tunnel experiments. The wind velocity of the surrounding flow field and the center of the opening were measured. The ventilation rate was obtained by tracer gas method with constant and continuous injection rate. The results showed that the oscillating frequency was independent of the opening separation except on the third floor probably because of the disturbance of the rooftop shedding frequency. The oscillating frequency on the first floor was the lowest due to the resistance of the ground to the vortex shedding. Pumping ventilation indicated that its ventilation rate is greater than that of general ventilation across the single opening with the same total opening area. The promotion of ventilation rate was up to about 123% on the first floor, about 65% on the second floor and about 44% on the third floor. Expansion of opening separations could boost the ventilation rate. Meanwhile, the fluctuation of opening center wind velocity and indoor species concentration were not positively correlated with the ventilation rate of pumping ventilation. Conclusions of this research could provide some useful reference to the design of natural ventilation for buildings.

Keywords

Pumping ventilation; Single-sided ventilation; Vortex shedding; Wind tunnel experiments; Natural ventilation

Main text

1. Introduction

1.1 Review of single-sided ventilation

Utilization of natural ventilation can largely save the energy consumption of mechanical ventilations in buildings (Chenari et al., 2016). Recently, due to impact of the ongoing respiratory COVID-19 pandemic, natural ventilation has been recommended to increase dilution of indoor air when environmental conditions and building requirements allow.

Natural ventilation can be divided into wind-driven and buoyancy-driven ventilation according to the driving force. In urban buildings with compact arrangements, windows are always arranged at the same elevation and not very large. In this case, the vertical pressure difference due to buoyancy at an opening becomes negligible compared the wind pressure difference across the window. As a result, buoyancy-driven ventilation becomes insignificant and wind force dominates the natural ventilation.

Cross ventilation (CV) and single-sided ventilation (SSV) are often considered as two main opening strategies of wind-driven ventilation. In urban buildings, SSV becomes increasingly more common than CV due to compact room arrangements and concerns of security and privacy (Allocca et al., 2003).

Methodologies that have been used on the study of SSV mainly included empirical equations (Cockroft and Robertson, 1976; Warren, 1977), airflow network models (Ai and Mak, 2014; Dascalaki et al., 1995), CFD simulations (Jiang and Chen, 2003; Jiang et al., 2003) and experiments (Gids and Phaff, 1982; Chu et al., 2015). Empirical equations and airflow network models can be very convenient to predict the ventilation rate of SSV but sometimes with unsatisfying accuracy. CFD simulations can provide more accurate results to some extent but its calculation accuracy still needs the validation by experiments (Jiang and Chen, 2003; Jiang et al., 2003; Yamanaka et al., 2006).

Therefore, experiments are the most convincing method of studying building ventilation and are often used to validate the reliability of other methods. Both full and reduced-scale experiments can be adopted to investigate SSV. Full-scale experiments often referred to field measurements, which take an advantage of in situ environmental condition and of no similarity problems. However, field measurements highly rely on the outdoor condition and may cause a high cost, thus are not always applicable. Reduced-scale experiments can be a cost-efficient and reliable way to study SSV as long as the similarity rules are properly obeyed. Boundary-layer wind tunnel experiment has become one of the most popular reduced-scale experiments on building ventilation study. It can reproduce a similar incident boundary layer as the real atmospheric boundary layer and achieve many unusual wind conditions as required (Cermak, 1999).

Wind tunnel experiments have been widely applied to research on SSV. SSV can be divided into SS1 (one opening) and SSn (multiple (n) openings) according to the opening number. According to literature, most wind tunnel experimental studies on SSV focused on SS1 (Jiang et al., 2003; Eftekhari et al., 2003; Kato et al., 2006; Yamanaka et al., 2006; Larsen and Heiselberg, 2008; Bu and Kato, 2011; Chu et al., 2011; Larsen et al., 2018). In these studies, wind velocity distribution and airflow rate through the opening were measured by Laser Doppler Anemometry (Jiang et al., 2003), hot wire anemometer (Bu and Kato, 2011), ultrasonic anemometer (Larsen and Heiselberg, 2008) and Particle Image Velocimetry (PIV) (Yamanaka et al., 2006). Ventilation rate were obtained mostly via tracer gas method (Kato et al., 2006; Yamanaka et al., 2006; Larsen and Heiselberg, 2008; Bu and Kato, 2011; Chu et al., 2011). On the other hand, wind tunnel experiments on SS2 were rarely conducted. Freire et al. (2013) validated the SS2 ventilation rate predicted by empirical models using the results of wind tunnel experiments and the ventilation rate was obtained through tracer gas decay method. Chu et al. (2015) also used tracer gas decay method to measure the exchange rate of SS2 in a wind tunnel and compared the exchange rate with that predicted by the orifice equation. They finally proposed a semi-empirical model to predict the exchange rate through incorporating the time-averaged pressure difference and pressure fluctuation.

However, single-sided ventilation rate was sometimes not able to satisfy the fundamental requirements of indoor air quality and comfort, especially in the period of COVID-19 pandemic. Common air conditioning without fresh air system may worsen the indoor cross infection of disease according to research (Lu et al., 2020). It is thus important to find a way to improve the ventilation rate and efficiency of single-sided ventilation.

1.2 Review of periodic vortex shedding and pumping ventilation

Pumping ventilation is a special wind-driven mechanism of single-sided ventilation, induced by the periodic vortex shedding at the building wake. It occurs when there are two openings on the same external wall and was first found by Daish et al. (2016) in their wind tunnel experiments. The oscillation frequency of the wake flow caused by vortex shedding can be quantified by a normalized parameter *St* (Strouhal number), expressed as $St = nW/U$, where n is the vortex shedding frequency, W is the bluff body width and U is the incident stream-wise velocity. Different *St* could be obtained for different bluff body geometry and *Re*.

Existing studies on vortex shedding can be divided into 2D and 3D. For 2D vortex shedding, *St* is between 0.07 and 0.21. *St* measured behind a square is around 0.13 (Okajima, 1982; Nakagawa, 1987; Knisely, 1990). For rectangular with different side ratios L/W (longitude length/latitude width), *St* is between 0.13 and 0.15 when $L/W < 1$ (Knisely, 1990) and then decreases from 0.12 to 0.07 when $1 < L/W < 2.5$ (Okajima, 1982; Knisely, 1990). When $2.5 < L/W < 3$, *St* changes discontinuously and ranges from 0.07 to 0.17 (Okajima, 1982; Knisely, 1990; Nakaguchi et al., 1968). For $3 < L/W < 8$, St decreases from 0.17 to 0.07 (Okajima, 1982; Knisely, 1990). After that, another discontinuous change occurred when $8 < L/W < 10$ (Knisely, 1990). For $10 < L/W < 25$, *St* decreases slowly from 0.19 to 0.16 with the increase of L/W (Knisely, 1990). Compared with 2D vortex shedding, *St* of 3D vortex shedding has a smaller range of 0.09-0.15. Specifically, *St* of a cube is between 0.09 and 0.10 (Tominaga et al., 2008; Liu & Niu, 2016; Wang et al., 2019; Hui et al., 2019) and *St* of a cuboid is 0.09-0.12 (Huang et al., 2007; Daish et al., 2016; Liu et al., 2017).

It is revealed that two or more openings have better ventilation effectivity than one for the same total opening area (Graça and Linden, 2016). Zhong et al. (2018) reproduced pumping flow through a rectangular building using 2D CFD simulation and considered the influence of upstream wind speed, side ratio of the building and opening separation on pumping frequency and ventilation rate. Considering that 2D simulations cannot predict real 3D flow structure, Zhong et al. (2019) then carried out 3D CFD simulations on the pumping ventilation of an infinite tall building. They found that pumping frequency and ventilation rate showed some different correlation with upstream wind velocity compared with 2D simulations and that pumping ventilation can also be observed when openings are mounted on the front wall. Further, Albuquerque et al. (2020) performed wind tunnel experiments and CFD simulations to investigate the ventilation mechanism of pumping ventilation. They visualized the flow field using smoke visualization and particle image velocimetry, and compared the effective ventilation rate of different window separations via tracer gas decay method. They found that the effective ventilation rate increased linearly with window separations

According to literature review on pumping ventilation through a single building, only the effect of upstream wind speed, side ratio of the building and opening separation were considered. For an urban building with many stories, behavior of pumping ventilation may be different on different floors. Thus, this paper performed wind tunnel experiments to study pumping ventilation with different opening separations on different floors, so as to provide some theoretical reference for promoting the ventilation rate of pumping ventilation and single-sided ventilation.

2. Methodology

2.1. Outline of wind tunnel

The experiments were conducted in the boundary layer wind tunnel at Institute of Industrial Science, the University of Tokyo (see **Fig. 1**). The test section had dimensions of 1.8 × 2.2 × 16.47 m^3 (height × width × length). The wind tunnel can provide adjustable inflow wind speed from 0.2 m/s to 20 m/s. Three vertical triangular spires and a large number of wooden cubes with dimensions of 3, 6 and 9 cm were placed upstream of the test section to generate and reproduce turbulence and the atmospheric boundary layer (ABL) profile.

Fig. 2 shows the profile of mean stream-wise velocity U and turbulence intensity I_u of approaching wind measured in the wind tunnel at the location of building center without building model. The velocity was measured by a constant-temperature hot wire anemometer, CT-HWA, with an X-wire probe (55P61, DANTEC). The mean wind velocity profile can be characterized by the power law:

$$\frac{U}{U_H} = (\frac{z}{H})^{\alpha} \quad (1)$$

where U_H is U at the building height H (In **Fig. 2**, U_H is 6.76 m/s), z is the height to the floor, and α is the power-law exponent (= 0.19).

2.2. Model and case description

The studied three-story model was a 1/30 reduce-scaled building with dimensions of 30 × 30 × 30 cm^3 ($H \times W \times W$). Each floor was 10 cm in height. For every ventilating case, only one floor was ventilated through one or two openings and the other two floors were sealed. **Fig. 3(a)** shows the building model of which the second floor was ventilated through two identical rectangular openings. As shown in **Fig. 3(b)**, width and height of each opening were both L_w (= 5 cm). The distance between the centerline of two openings was S, and the dimensionless opening separation was defined as $s' = S/W$.

The case arrangement considering different influencing factors on pumping ventilation is presented in **Table 1**. U_H was the same for all cases. Cases with no opening (s' = /) were included to clarify the effect of openings on the flow field around the building. s' = 0 refers to SS1. s' = 0.25, 0.50 and 0.75 refers to the three different opening separations for SS2 cases. In the following sections, a simplified form [s', floor] will be used to denote each case.

The formation of the pumping ventilation is due to the periodic vortex shedding induced by the instability of the two shear layer from the building sides. According to our former publications on pumping ventilation, the periodicity of pumping flow was clearly observed for a large range of *Re* from 1.1×10^5 to 8.75×10^7 considered in our former studies (Zhong et al., 2018, 2019a, 2019b, 2020). It is widely accepted that the mean flow characteristics will be similar if the Reynolds number is large enough (Townsend, 1956). The Reynolds number of the approaching flow based on the building height length scale was 120000, which was sufficiently larger than the recommended *Re* (> 4000) by Castro and Robins (1977) and also larger than the conservative *Re* (> 11000) suggested by Snyder (1981). Moreover, Tominaga and Stathopoulos (2018) confirmed that the difference was negligible between the measured velocities for *Re* = 5700 and that for *Re* = 57000 in wind tunnel experiments. Therefore, the flow field around the building in the present study could be considered self-similar with that in full-scale condition. Besides, the independence of *Re* inside the building of SSV can be expressed by *Re* based on the opening width scale, which was 20000 in this study. Kato et al. (2006) conducted wind tunnel experiments for SS1 and *Re* was 4700 based on the length scale of the opening width. Similarly, *Re* was between 5400 and 27000 in the experiments of Chu et al. (2011). In the most recent wind tunnel experiments of SS2 of a 1/20 scaled building (Albuquerque et al., 2020), *Re* of the reduced-scale building model was about 17500 based on the opening scale. Therefore, the flow field inside the building of SSV in this study was also supposed to be self-similar with that in full-scale condition.

2.3. Velocity measurements

The velocity measurements included the stream-wise instantaneous velocity at the right-side opening center point (also referred as u_w hereafter) and mean velocity distribution in the wake region of the building (U_x). Wind velocity was measured using a constant-temperature hot wire anemometer (CT-HWA) with a split-fiber probe (SFP), (55R55, DANTEC). The SFP can measure the adverse velocity for a wind direction. The

CT-HWA can measure the wind velocity from 0.02 to 300 m/s. The measuring accuracy depends on the calibration accuracy, which is typically around 0.5% and will not exceed 2%. The response time is short enough and can be negligible. The CT-HWA also enables accurate measurement of frequency up to 100 kHz and thus is sufficient for the measurement of pumping ventilation frequency.

A coordinate axis was defined and the coordinate origin is located at the center point of the bottom side of the rear surface (see **Fig. 3**). To measure the stream-wise velocity, the probe wire was placed horizontally, perpendicular to the stream-wise direction (see **Fig. 4**). Each measurement's period time was 120 s at a frequency of 1000 Hz, obtaining totally 1.2×10^5 sampling data. **To test the stability of the wind tunnel, normalized standard deviation of measured opening center velocity u_w for different measuring period time of case [s', floor] = [0.5, 2] is listed in Table 2. It is observed that the deviations between different sampling period times were lower than 1.00%, which could be negligible. Therefore it is believed that the velocity measurement was reliable and repeatable in the wind tunnel experiments.**

2.4. Frequency of pumping flow

We defined the pumping flow frequency as the frequency of the stream-wise wind velocity at the opening center point. From fast Fourier transform (FFT) of the velocity time history, we could obtain the dominant frequency *n* (Hz) corresponding to the peak of the power spectrum density (PSD) (see **Fig. 5**). Strouhal number was often used to denote the normalized vortex shedding frequency at the wake of a building (Lyn et al., 1995; Chen and Liu, 1999; Liu and Niu, 2016) and is nearly independent of *Re* between 10000 and 200000. In the present study, we also use this way to normalize the oscillation frequency of pumping flow of each floor and opening separation. The normalized pumping flow frequency St_w is defined as

$$St_w = nH/U_H \qquad (2)$$

where *n* is the pumping flow frequency across the openings.

2.5. Ventilation rates

Measuring the airflow rate of a building model in the wind tunnel experiments is a difficult task. Instead, effective ventilation rates have been adopted by many researchers to quantify the ventilation effectiveness using tracer gas method (Albuquerque et al., 2020). In this study, ethylene (C_2H_4) was chosen as the tracer gas, mixed with nitrogen (N_2) to ensure security. The tracer gas was injected continuously at a total flow rate of 2 L/min (1.21 % C_2H_4) from 8 evenly spaced vertical rods (see Fig. 3(a), (c) and (d)). Each injection rod was half the height of the floor (H/6 = 5 cm). The concentrations were sampled using a fast flame ionization detector (FID) at the center point of the room, with a period of 120 s and at a frequency of 1000 Hz. **In the FID, negative ions are produced when hydrocarbons (C2H4) is burn. This ion is captured by the high voltage electrode, and the generated current is detected as an electric signal. The amount of generated ions is proportional to the number of carbon atoms in the burned hydrocarbon, so that the electrical signal and the hydrocarbon concentration in the sample gas are associated. H_2 and air are introduced into a burner frame as fuel gas to produce the above combustion reaction.** Each sampling period began 120 s after the tracer gas injection was started, to ensure a complete mixing of the tracer gas within the ventilated floor. FID can measure the concentration of tracer gas from 10 mV/ppm to 10 V/ppm and the response time is about several msec. **For concentration sampling of each case, measurements were conducted three times repeatedly and the arithmetic mean values of three repeated samplings were obtained.**

Purging flow rate (*PFR*) was adopted as the effective ventilation rate of the building model (Sandberg and Sjöberg, 1983). *PFR* quantifies the rate at which pollutants are removed from a homogeneously mixed region and thus can express the pollutant removal capability of a ventilation system. *PFR* can be obtained in the experiments as follows (Awbi, 2003):

$$PFR = \frac{Q}{\langle c \rangle} \tag{3}$$

where Q (L/min) is the injection rate of the tracer gas C_2H_4 and $\langle c \rangle$ represents the temporal spatial averaged concentration of C_2H_4 in the ventilated room. Since we assumed that the tracer gas in the ventilated room is completely mixed before sampling, the measured concentration by FID could be considered as the average equilibrium concentration in the room (Kato et al., 2006). $\langle c \rangle$ was finally calculated as the time-averaged value of the sampling period. The reference concentration c_0 was defined as

$$c_0 = \frac{Q}{H^2 U_H} \tag{4}$$

In order to remove the effect of room volume, air change per hour (*ACH*) was often used to evaluate the ventilation rate of building ventilation (Argiriou et al., 2002; Larsen and Heiselberg, 2008). Here we used ACH_{PFR} to define the air change rate (s^{-1}) of the ventilated floor based on *PFR* as follows:

$$ACH_{PFR} = \frac{PFR}{V_{room}} \tag{5}$$

where V_{room} (m^3) is the internal volume of the ventilated floor. ACH_{PFR} will also be referred as ventilation rate hereafter.

3. Results

3.1. Velocity distribution

To study the influence of openings on the velocity distribution in the wake region of the isolated building, three different cases, i.e. [s', floor] = [/, /] (no opening), [0, 2] (SS1) and [0.50, 2] (SS2), were considered. The stream-wise velocity (U_x) were measured and averaged at measuring points on three different vertical lines (x/H = 0.07, 0.125, 0.250, y/H = 0) and horizontal lines (x/H = 0.07, 0.125, 0.250, z/H = 0.5)， which were in the near wake region. In this region, the effect of the leeward façade openings on the flow characteristics could be the most significant. Each vertical/horizontal line had 8/9 measuring points respectively (see **Fig. 6**). **Fig. 6** reveals that the vertical and horizontal distributions of U_x for three cases were almost the same even for the measurement line that was closest to the leeward wall (x/H = 0.07). This is probably because that the openings were not very large openings and will not apparently affect the wake region flow characteristics. Therefore, the number of openings has negligible effects on the stream-wise velocity in the wake region of the building if the openings are not large enough.

3.2. Pumping flow frequency

The time histories of the stream-wise wind velocity u_w at the opening center of case [0, 2] (SS1) and [0.50, 2] (SS2) are shown in **Fig. 7**. u_w in SS2 showed more regular periodic oscillation than SS1 though periodic oscillation can be seen from both SS1 and SS2.

The oscillation frequency of pumping flow is represented by the St_w (**Eq. (2)**), normalized by U_H and H. The effect of opening separations (s') to St_w on different floors has been presented in **Fig. 8**. The range of St_w is generally between 0.12 and 0.54. For SS1, since the pumping flow does not exist, St_w of SS1 was not calculated. As illustrated in **Fig. 8**, St_w was nearly constant for the same floor and independent of the opening separation, i.e. about 0.12 on the first floor and about 0.16 on the second floor. The independence of pumping flow frequency from the opening separation was also reported by Zhong et al. (Zhong et al., 2019). For the third floor, St_w for the other two opening separations were also nearly the same and close to that on the second floor except the relatively larger St_w for $s' = 0.25$. It was probably because of the interference of another kind of vortex shedding (e.g. rooftop shedding or arch-type vortex shedding (Zhang et al., 2020), which suppressed the horizontal vortex shedding from the sidewalls and dominated the oscillating frequency at the rear openings. Due to the resistance of the ground to the periodic vortex shedding from the building, St_w was the lowest on the first floor for all s'. From the first to the upper floors, since the effect of ground becomes insignificant, the St_w got larger but no longer rised from the second to the third floor for $s' = 0.50$ and 0.75. Different floor corresponds to different frequency, which indicates that the pumping flow frequency is not always equals to the vortex shedding frequency considering different ventilating floors. St_w on the first floor is the closest to ($St = 0.12$) that reported by Liu & Niu (2016).

3.3. Ventilation rate

ACH_{PFR} of both SS1 and SS2 were calculated from **Eq. (5)**. **Fig. 9** shows the variation of ACH_{PFR} for different s' and floors. ACH_{PFR} on the first floor was the largest while that on the third floor was the smallest. As illustrated in **Fig. 8**, St_w at the openings on the first floor was the lowest. We can then deduce that the ventilation rate doesn't have a positive correlation with the pumping flow frequency. This conclusion was also supported in Zhong et al. (2020). On the whole, ACH_{PFR} is promoted when increasing the opening separation on the second and third floors, as reported in the former study (Zhong et al., 2019). However, there was a reduction of ACH_{PFR} from $s' = 0.50$ to 0.75 on the first floor, indicating that increasing the opening separation cannot necessarily promote the ventilation rate when the openings are on the first floor close to the ground surface. Nevertheless, the ventilation rate of SS2 was always larger than that of SS1 ($s' = 0$) with the same total opening area. ACH_{PFR} can be increased by up to about 123% compared with SS1 on the first floor ($s' = 0.50$), about 65% on the second floor and about 44% on the third floor.

3.4. Velocity and concentration fluctuations

Turbulent fluctuations could dominate the airflow field characteristics and air exchange of SSV for many wind directions (Furbringer and Maas, 1995; Chu et al., 2011). Velocity fluctuations across the opening thus played an important role in the ventilation rate. The center zone of a building is usually the most concerned occupied zone, thus the concentration fluctuation at the building center was measured to quantify the variation characteristics at that point. The time history of C_2H_4 concentration for case [0.5, 2] is shown in Fig. 10(a). It can be observed that the concentration shows nearly periodic variation with time.

The standard deviation (SD) of the stream-wise wind velocity at the opening center SD_u was normalized by U_H ($\sigma_u = SD_u/U_H$) and the SD of C_2H_4 concentration SD_c was normalized by c_0 ($\sigma_c = SD_c/c_0$).

The correlation between σ_u and s' differed a lot from that between ACH_{PFR} and s'. σ_u reached its maximum values at lower opening separations, i.e. $s' = 0.25$ or 0.50, and relatively lower σ_u occurred at the largest opening separation ($s' = 0.75$) and SS1 ($s' = 0$). σ_u on the first and third floors were the largest and smallest, respectively (see **Fig. 10 (b)**).

The correlation between the concentration fluctuation and the opening separation on different floors is presented in **Fig. 10 (c).** σ_c on the first floor was the most sensitive to s' and decreased rapidly with the increase of s' while σ_c on the second and third floors were less affected by s'. For SS2, the concentration fluctuation of the second floor was the largest while which floor had the lowest σ_c depended on the opening separation and could not be simply concluded. However, the ventilation rate on the third floor was the lowest. It can be found that the ventilation rate and σ_c were not positively correlated for pumping ventilation.

As σ_c could not express the relative instability of concentration for different cases, concentration fluctuation intensity was adopted, normalizing the standard deviation of concentration by mean concentration (Lin et al., 2020). It expresses the relative instability of the concentration and is defined as $I_c = \sigma_c/\langle c \rangle$.

The concentration fluctuation intensity at different opening separations is shown in **Fig. 11**. For SS2 ($s' \geq 0.25$), the instability of concentration was strengthened when opening separation s' became larger on the second and third floors. However, it became stable when s' increased on the first floor, in compliance with the results that the ventilation rate also decreased at larger opening separation on the first floor.

I_c on the third floor was the most stable among the three different floors. We can also find from **Fig. 10 (b)** that σ_u on the third floor was the lowest, indicating that the pumping flow on the third floor, i.e. the top floor, was the most insignificant. This result also consists with that in Sec. 3.3, reporting that the lowest ventilation rate ACH_{PFR} occurred on the third floor. The insignificance of pumping flow on the third floor was probably due to the fact that pumping flow could be easily disturbed by the roof shedding flows.

Fig. 12 presents the probability density function (PDF) of concentration for different opening separations *s′*, and ventilated floors. The horizontal coordinate value denotes the degree of deviation from average concentration. The positive deviation was always larger than the negative deviation. The positive deviation for *s′* = 0.25 was the largest among four *s′* (**Fig. 12 (a)**). Both the negative and the positive deviation of the second floor were the largest among three floors (**Fig. 12 (b)**).

4. Discussion

This research investigated the pumping ventilation on different floors, which was not considered in former publications. Literature review indicated that former ones only discussed about the pumping flow on the middle floor or through openings located at the middle height of the building. The pumping ventilation was much "purer" and less affected by the ground or the rooftop shedding flows on the middle floors. However, as investigated in this paper, St_w on the first floor and ACH_{PFR} on the third floor sometimes showed different correlation with the opening separations. Hence, the existing rules concluded by past investigations of pumping ventilation may not be applicable for all floors of a multi-story building, especially on the bottom and the top floors.

Certainly, present study on pumping ventilation was still limited in the ideal and theoretical level. As pumping ventilation is mostly a horizontal wind behavior, the vertical mutual influence may not be significant. Nevertheless, it would certainly be better if the openings on every floor are opened to consider the mutual influence between openings on different floors, which will be included in our further studies. In addition, the contribution of the velocity fluctuations to the ventilation rate of pumping ventilation still need to be quantified with the help of CFD simulation. The present experimental study on pumping ventilation is still an early stage of the pumping ventilation study in the real buildings in urban areas.

5. Conclusions

This study presented wind tunnel experiments on the pumping ventilation of an isolated three-story building model. Opening separation and ventilated floor represented main influencing factors. The wind velocity was measured by CT-HWA and the ventilation rate was represented by ACH_{PFR} and obtained using tracer-gas method. Main conclusions were summarized as follows,

(1) St_w was independent of the opening separation on the first and second floor except an extraordinary large St_w on the third floor probably because of the disturbance of the rooftop shedding frequency. *St* on the first floor became the lowest due to the effect of the ground to the vortex shedding.

(2) The ventilation rate (ACH_{PFR}) of SS2 was always higher than that of SS1 with the same total opening area. The ventilation rate could be promoted by increasing the opening separation while on the first floor the ventilation rate may start to decrease for large opening separation. The ventilation rate on the first floor was the highest while that on the third floor became the smallest. ACH_{PFR} could be increased up to about 123% comparing with that of SS1 on the first floor, about 65% on the second floor and about 44% on the third floor.

(3) Neither the opening center wind velocity fluctuation nor the indoor concentration fluctuation was positively correlated with the ventilation rate of pumping ventilation. The response of velocity and concentration fluctuation to the opening separation and ventilated floor were not consistent.

(4) The conclusion of this study can be applied to generic building configurations and may be no longer applicable for buildings with other different shapes, structures or for buildings with very large openings. The pumping ventilation for more building configurations still requires further investigation in the following studies.

Acknowledgements

This research was financially supported by the ***Natural Science Foundation of China*** (NSFC Grant No. 51778504; Grant No. U1867221), ***Science and Technology Innovation Leader of Hunan Province*** (Grant No. 2020RC4032, Hunan University of Technology), ***Fundamental Research Funds for the Central Universities*** (Grant No. 2042020kf0203, Wuhan University), and ***National Key Research and Development Program of the Ministry of Science and Technology of China*** (Grant No. 2018YFC0705201, Grant No. 2018YFB0904200).

References

B. Chenari, J. Carrilho, M. Silva. Towards sustainable, energy-efficient and healthy ventilation strategies in buildings: A review, ***Renewable and Sustainable Energy Reviews***, 59 (2016) 1426-1447.

C. Allocca, Q.Y. Chen, L.R. Glicksman. Design analysis of single–sided natural ventilation, ***Energy and Buildings***, 35 (2003) 785-795.

J.P. Cockroft, P. Robertson. Ventilation of an enclosure through a single opening, ***Building and Environment*** 11 (1976) 29-35.

P.R. Warren. Ventilation through openings on one wall only. In International Centre for Heat and Mass Transfer Conference: Energy Conservation in Heating, Cooling and Ventilating Buildings; Hoogendorn, C.J., Afgar, N.H., Eds.; Hemisphere Publishing Corporation: Dubrovnik, Yugoslavia, 1977; Volume 1, pp. 189–209.

Z.T. Ai, C.M. Mak. Determination of single-sided ventilation rates in multistory buildings: Evaluation of methods, ***Energy and Buildings*** 69 (2014) 292-300.

E. Dascalaki, M. Santamouris, A. Argiriou et al. Predicting single sided natural ventilation rates in buildings, ***Solar Energy*** 55 (1995) 327-341.

Y. Jiang, Q. Chen. Buoyancy-driven single-sided natural ventilation in buildings with large openings, ***International Journal of Heat and Mass Transfer*** 46 (2003) 973-988.

Y. Jiang, D. Alexander, H. Jenkins, R. Arthur, Q. Chen. Natural ventilation in buildings: measurement in a wind tunnel and numerical simulation with large-eddy simulation, ***Journal of Wind Engineering and Industrial Aerodynamics*** 91 (2003) 331-353.

W.De Gids, H. Phaff. Ventilation rates and energy consumption due to open windows, ***Air Infiltration Review*** 4 (1982) 4-5.

C.R. Chu, Y.H. Chiu, Y.T. Tsai, S.-L. Wu. Wind-driven natural ventilation for buildings with two openings on the same external wall, ***Energy and Buildings*** 108 (2015) 365-372.

J. Cermak. Wind tunnel studies of buildings and structures, ***American Society of civil engineers***, 1999.

M.M. Eftekhari, L.D. Marjanovic, D.J. Pinnock. Air flow distribution in and around a single-sided naturally ventilated room, ***Building and Environment*** 38 (2003) 389-397.

S. Kato, R. Kono, T. Hasama, R. Ooka, T. Takahashi. A wind tunnel experimental analysis of the ventilation characteristics of a room with single-sided opening in uniform flow, ***International Journal of Ventilation*** 5 (2006) 171-178.

T. Yamanaka, H. Kotani, K. Iwamoto, M. Kato. Natural, wind-forced ventilation caused by turbulence in a room with a single opening, ***International Journal of Ventilation*** 5 (2006) 179-187.

T.S. Larsen, P. Heiselberg. Single-sided natural ventilation driven by wind pressure and temperature difference, ***Energy and Buildings*** 40 (2008) 1031-1040.

Z. Bu, S Kato. Wind-induced ventilation performances and airflow characteristics in an areaway-attached basement with a single-sided opening, ***Building and Environment*** 46 (2011) 911-921.

C.R. Chu, R.-H. Chen, J.-W. Chen. A laboratory experiment of shear-induced natural ventilation, ***Energy and Buildings*** 43 (2011) 2631–2637.

R. Freire, M. Abadie, N. Mendes. On the improvement of natural ventilation models, ***Energy and Buildings*** 62 (2013) 222-229.

T. Larsen, C. Plesner, V. Leprince, F. Carrié, A. Bejder. Calculation methods for single-sided natural ventilation: Now and ahead, ***Energy and Buildings*** 177 (2018) 279-289.

J. Lu, J. Gu, K. Li et al. COVID-19 Outbreak Associated with Air Conditioning in Restaurant, Guangzhou, China, 2020, ***Emerging Infectious Diseases*** 26 (2020) 1628-1631.

N.C. Daish, G. Carrilho da Graça, P.F. Linden, D. Banks. Impact of aperture separation on wind-driven single-sided natural ventilation, ***Building and Environment*** 108 (2016) 122-134.

G. Carrilho da Graça, P. Linden. Ten questions about natural ventilation of non-domestic buildings, ***Building and Environment*** 107 (2016) 263-273.

H. Zhong, D.D. Zhang, D. Liu, F.Y. Zhao, Y.G. Li, H.Q. Wang. Two dimensional numerical simulation of wind driven ventilation across a building enclosure with two free apertures on the rear side: Vortex shedding and "pumping flow mechanism", ***Journal of Wind Engineering and Industrial Aerodynamics*** 179 (2018) 449–462.

A.A.R. Townsend. The Structure of Turbulent Shear Flow. Cambridge university press, 1956.

I.P. Castro, A.G. Robins. The flow around a surface-mounted cube in uniform and turbulent streams. ***Journal of Fluid Mechanics*** 79 (1977) 307-335.

W.H. Snyder. *Guideline for Fluid Modeling of Atmospheric Diffusion*, 1981.

Y. Tominaga, T. Stathopoulos. CFD simulations of near-field pollutant dispersion with different plume buoyancies, ***Building and Environment*** 131 (2018) 128-139.

D. Albuquerque, M. Sandberg, P. Linden, G. Carrilho da Graça. Experimental and numerical investigation of pumping ventilation on the leeward side of a cubic building, ***Building and Environment*** 179 (2020) 106897.

A.A. Argiriou, C.A. Balaras, S.P. Lykoudis. Single-sided ventilation of buildings through shaded large openings, ***Energy*** 27 (2002) 93-115.

B. Zhang, R. Ooka, H. Kikumoto. Analysis of turbulent structures around a rectangular prism building model using spectral proper orthogonal decomposition, ***Journal of Wind Engineering & Industrial Aerodynamics*** 206 (2020) 104213.

H. Zhong, D. Zhang, Y. Liu, D. Liu, F. Zhao, Y. Li, H. Wang. Wind driven "pumping" fluid flow and turbulent mean oscillation across high-rise building enclosures with multiple naturally ventilated apertures, ***Sustainable Cities and Society*** 50 (2019) 101619.

H. Zhong, Y. Jing, Y. Liu, F. Zhao, D. Liu, Y. Li. CFD simulation of "pumping" flow mechanism of an urban building affected by an upstream building in high Reynolds flows, ***Energy and Buildings*** 202 (2019) 109330.

H. Zhong, Y. Jing, Y. Sun, H. Kikumoto, F. Zhao, Y. Li. Wind-driven pumping flow ventilation of highrise buildings: Effects of upstream building arrangements and opening area ratios, ***Science of the Total Environment*** 722 (2020) 137924.

Chao Lin, Ryozo Ooka, Hideki Kikumoto, Taiki Sato, Maiko Arai. Wind tunnel experiment on high-buoyancy gas dispersion around isolated cubic building, ***Journal of Wind Engineering & Industrial Aerodynamics*** 202 (2020) 104226.

D.A. Lyn, S. Einav, W. Rodi, J.H. Park, A laser-Doppler velocimetry study of ensemble-averaged characteristics of the turbulent near wake of a square cylinder, ***Journal of Fluid Mechanics*** 304 (1995) 285-319.

J.M. Chen, C.H. Liu, Vortex shedding and surface pressures on a square cylinder at incidence to a uniform air stream, ***International Journal of Heat and Fluid Flow*** 20 (1999) 592-597.

J. Liu, J. Niu. CFD simulation of the wind environment around an isolated high-rise building: An evaluation of SRANS, LES and DES models, ***Building and Environment*** 96 (2016) 91-106.

M. Sandberg, M. Sjöberg. The use of moment for assessing air quality in ventilated rooms, ***Building and Environment*** 18 (1983) 181–97.

H. Awbi. Ventilation of buildings. Taylor & Francis, 2003.

J. Furbringer, J. Maas. Suitable algorithms for calculating air renewal rate by pulsating air flow through a single large opening, ***Building and Environment*** 30 (1995) 493-503.

A. Okajima. Strouhal Numbers of Rectangular Cylinders, ***Journal of Fluid Mechanics*** 123 (1982) 379-398.

T. Nakagawa. Vortex shedding behind a square cylinder in transonic flows, ***Journal of Fluid Mechanics*** 178 (1987) 303-323.

C.W. Knisely. Strouhal numbers of rectangular cylinders at incidence: a review and new data, ***Journal of Fluid and Structures*** 4 (1990) 371–393.

H. Nakaguchi, K. Hashimoto, S. Muto. An experimental study on aerodynamic drag of rectangular cylinders, ***The Journal of the Japan Society of Aeronautical Engineering*** 16 (1968) 1-5.

Y. Tominaga, A. Mochida, S. Murakami, S. Sawaki. Comparison of various revised k-ε models and LES applied to flow around a high-rise building model with 1:1:2 shape placed within the surface boundary layer, ***Journal of Wind Engineering and Industrial Aerodynamics*** 96 (2008) 389-411.

J. Liu, J. Niu. CFD simulation of the wind environment around an isolated high-rise building: an evaluation of SRANS, LES and DES models, ***Building and Environment*** 96 (2016) 91-106.

F. Wang, K.M. Lam, G.B. Zu, L. Cheng. Coherent structures and wind force generation of square-section building model, ***Journal of Wind Engineering and Industrial Aerodynamics*** 188 (2019) 175-193.

Y. Hui, K. Yuan, Z. Chen, Q. Yang. Characteristics of aerodynamic forces on high-rise buildings with various façade appurtenances, Journal of Wind Engineering and Industrial Aerodynamics 191 (2019) 76-90.

S. Huang, Q.S. Li, S. Xu. Numerical evaluation of wind effects on a tall steel building by CFD, ***Journal of Constructional Steel Research*** 63 (2007) 612-627.

J. Liu, J. Niu, C.M. Mak, Q. Xia. Detached eddy simulation of pedestrian-level wind and gust around an elevated building, ***Building and Environment*** 125 (2017) 168-179.

Manuscript

Boundary Layer Wind Tunnel Modeling Experiments on Pumping Ventilation through a Three-Story Reduce-Scaled Building with Two Openings

Huai-Yu Zhong[1,2#], Chao Lin[3,4#], Yang Sun[5], Hideki Kikumoto[4], Ryozo Ooka[4], Hong-Liang Zhang[1,2], Hong Hu[3,4], Fu-Yun Zhao[1,2]*, Carlos Jimenez-Bescos[6]

(1) Key Laboratory of Hydraulic Machinery Transients (***Wuhan University***), Ministry of Education, Wuhan, Hubei Province, P. R. China

(2) School of Power and Mechanical Engineering, ***Wuhan University***, Wuhan, Hubei Province, P. R. China

(3) Graduate School of Engineering, ***The University of Tokyo***, 4-6-1 Komaba, Meguro-ku, Tokyo, 153-8505, Japan

(4) Institute of Industrial Science, ***The University of Tokyo***, 4-6-1 Komaba, Meguro-ku, Tokyo, 153-8505, Japan

(5) Department of Mechanical Engineering, ***Wanjiang University of Technology***, Ma-An-Shan, Anhui Province, P. R. China

(6) Department of Architecture and Built Environment, ***University of Nottingham***, Nottingham, UK

[#] These two authors contributed equally and should be regarded as co-first authors.

* Corresponding author:

Prof. Fu-Yun Zhao

Address: School of Power and Mechanical Engineering, Wuhan University, Wuhan, Hubei Province, P. R. China

Emails: fyzhao@whu.edu.cn, zfycfdnet@163.com

Abstract and keywords

Abstract

Pumping ventilation is a special single-sided wind driven building ventilation induced by periodic vortex shedding at the building wake. This work aimed to investigate the oscillating frequency at the building façade opening and ventilation rate of pumping ventilation. The effects of opening separations on different floors of a three-story reduce-scaled building with two openings were considered using boundary-layer wind tunnel experiments. The wind velocity of the surrounding flow field and the center of the opening were measured. The ventilation rate was obtained by tracer gas method with constant and continuous injection rate. The results showed that the oscillating frequency was independent of the opening separation except on the third floor probably because of the disturbance of the rooftop shedding frequency. The oscillating frequency on the first floor was the lowest due to the resistance of the ground to the vortex shedding. Pumping ventilation indicated that its ventilation rate is greater than that of general ventilation across the single opening with the same total opening area. The promotion of ventilation rate was up to about 123% on the first floor, about 65% on the second floor and about 44% on the third floor. Expansion of opening separations could boost the ventilation rate. Meanwhile, the fluctuation of opening center wind velocity and indoor species concentration were not positively correlated with the ventilation rate of pumping ventilation. Conclusions of this research could provide some useful reference to the design of natural ventilation for buildings.

Keywords

Pumping ventilation; Single-sided ventilation; Vortex shedding; Wind tunnel experiments; Natural ventilation

Main text

1. Introduction

1.1 Review of single-sided ventilation

Utilization of natural ventilation can largely save the energy consumption of mechanical ventilations in buildings (Chenari et al., 2016). Recently, due to impact of the ongoing respiratory COVID-19 pandemic, natural ventilation has been recommended to increase dilution of indoor air when environmental conditions and building requirements allow.

Natural ventilation can be divided into wind-driven and buoyancy-driven ventilation according to the driving force. In urban buildings with compact arrangements, windows are always arranged at the same elevation and not very large. In this case, the vertical pressure difference due to buoyancy at an opening becomes negligible compared the wind pressure difference across the window. As a result, buoyancy-driven ventilation becomes insignificant and wind force dominates the natural ventilation.

Cross ventilation (CV) and single-sided ventilation (SSV) are often considered as two main opening strategies of wind-driven ventilation. In urban buildings, SSV becomes increasingly more common than CV due to compact room arrangements and concerns of security and privacy (Allocca et al., 2003).

Methodologies that have been used on the study of SSV mainly included empirical equations (Cockroft and Robertson, 1976; Warren, 1977), airflow network models (Ai and Mak, 2014; Dascalaki et al., 1995), CFD simulations (Jiang and Chen, 2003; Jiang et al., 2003) and experiments (Gids and Phaff, 1982; Chu et al., 2015). Empirical equations and airflow network models can be very convenient to predict the ventilation rate of SSV but sometimes with unsatisfying accuracy. CFD simulations can provide more accurate results to some extent but its calculation accuracy still needs the validation by experiments (Jiang and Chen, 2003; Jiang et al., 2003; Yamanaka et al., 2006).

Therefore, experiments are the most convincing method of studying building ventilation and are often used to validate the reliability of other methods. Both full and reduced-scale experiments can be adopted to investigate SSV. Full-scale experiments often referred to field measurements, which take an advantage of in situ environmental condition and of no similarity problems. However, field measurements highly rely on the outdoor condition and may cause a high cost, thus are not always applicable. Reduced-scale experiments can be a cost-efficient and reliable way to study SSV as long as the similarity rules are properly obeyed. Boundary-layer wind tunnel experiment has become one of the most popular reduced-scale experiments on building ventilation study. It can reproduce a similar incident boundary layer as the real atmospheric boundary layer and achieve many unusual wind conditions as required (Cermak, 1999).

Wind tunnel experiments have been widely applied to research on SSV. SSV can be divided into SS1 (one opening) and SSn (multiple (n) openings) according to the opening number. According to literature, most wind tunnel experimental studies on SSV focused on SS1 (Jiang et al., 2003; Eftekhari et al., 2003; Kato et al., 2006; Yamanaka et al., 2006; Larsen and Heiselberg, 2008; Bu and Kato, 2011; Chu et al., 2011; Larsen et al., 2018). In these studies, wind velocity distribution and airflow rate through the opening were measured by Laser Doppler Anemometry (Jiang et al., 2003), hot wire anemometer (Bu and Kato, 2011), ultrasonic anemometer (Larsen and Heiselberg, 2008) and Particle Image Velocimetry (PIV) (Yamanaka et al., 2006). Ventilation rate were obtained mostly via tracer gas method (Kato et al., 2006; Yamanaka et al., 2006; Larsen and Heiselberg, 2008; Bu and Kato, 2011; Chu et al., 2011). On the other hand, wind tunnel experiments on SS2 were rarely conducted. Freire et al. (2013) validated the SS2 ventilation rate predicted by empirical models using the results of wind tunnel experiments and the ventilation rate was obtained through tracer gas decay method. Chu et al. (2015) also used tracer gas decay method to measure the exchange rate of SS2 in a wind tunnel and compared the exchange rate with that predicted by the orifice equation. They finally proposed a semi-empirical model to predict the exchange rate through incorporating the time-averaged pressure difference and pressure fluctuation.

However, single-sided ventilation rate was sometimes not able to satisfy the fundamental requirements of indoor air quality and comfort, especially in the period of COVID-19 pandemic. Common air conditioning without fresh air system may worsen the indoor cross infection of disease according to research (Lu et al., 2020). It is thus important to find a way to improve the ventilation rate and efficiency of single-sided ventilation.

1.2 Review of periodic vortex shedding and pumping ventilation

Pumping ventilation is a special wind-driven mechanism of single-sided ventilation, induced by the periodic vortex shedding at the building wake. It occurs when there are two openings on the same external wall and was first found by Daish et al. (2016) in their wind tunnel experiments. The oscillation frequency of the wake flow caused by vortex shedding can be quantified by a normalized parameter *St* (Strouhal number), expressed as $St = nW/U$, where n is the vortex shedding frequency, W is the bluff body width and U is the incident stream-wise velocity. Different *St* could be obtained for different bluff body geometry and *Re*.

Existing studies on vortex shedding can be divided into 2D and 3D. For 2D vortex shedding, *St* is between 0.07 and 0.21. *St* measured behind a square is around 0.13 (Okajima, 1982; Nakagawa, 1987; Knisely, 1990). For rectangular with different side ratios L/W (longitude length/latitude width), *St* is between 0.13 and 0.15 when $L/W < 1$ (Knisely, 1990) and then decreases from 0.12 to 0.07 when $1 < L/W < 2.5$ (Okajima, 1982; Knisely, 1990). When $2.5 < L/W < 3$, *St* changes discontinuously and ranges from 0.07 to 0.17 (Okajima, 1982; Knisely, 1990; Nakaguchi et al., 1968). For $3 < L/W < 8$, St decreases from 0.17 to 0.07 (Okajima, 1982; Knisely, 1990). After that, another discontinuous change occurred when $8 < L/W < 10$ (Knisely, 1990). For $10 < L/W < 25$, *St* decreases slowly from 0.19 to 0.16 with the increase of L/W (Knisely, 1990). Compared with 2D vortex shedding, *St* of 3D vortex shedding has a smaller range of 0.09-0.15. Specifically, *St* of a cube is between 0.09 and 0.10 (Tominaga et al., 2008; Liu & Niu, 2016; Wang et al., 2019; Hui et al., 2019) and *St* of a cuboid is 0.09-0.12 (Huang et al., 2007; Daish et al., 2016; Liu et al., 2017).

It is revealed that two or more openings have better ventilation effectivity than one for the same total opening area (Graça and Linden, 2016). Zhong et al. (2018) reproduced pumping flow through a rectangular building using 2D CFD simulation and considered the influence of upstream wind speed, side ratio of the building and opening separation on pumping frequency and ventilation rate. Considering that 2D simulations cannot predict real 3D flow structure, Zhong et al. (2019) then carried out 3D CFD simulations on the pumping ventilation of an infinite tall building. They found that pumping frequency and ventilation rate showed some different correlation with upstream wind velocity compared with 2D simulations and that pumping ventilation can also be observed when openings are mounted on the front wall. Further, Albuquerque et al. (2020) performed wind tunnel experiments and CFD simulations to investigate the ventilation mechanism of pumping ventilation. They visualized the flow field using smoke visualization and particle image velocimetry, and compared the effective ventilation rate of different window separations via tracer gas decay method. They found that the effective ventilation rate increased linearly with window separations

According to literature review on pumping ventilation through a single building, only the effect of upstream wind speed, side ratio of the building and opening separation were considered. For an urban building with many stories, behavior of pumping ventilation may be different on different floors. Thus, this paper performed wind tunnel experiments to study pumping ventilation with different opening separations on different floors, so as to provide some theoretical reference for promoting the ventilation rate of pumping ventilation and single-sided ventilation.

2. Methodology

2.1. Outline of wind tunnel

The experiments were conducted in the boundary layer wind tunnel at Institute of Industrial Science, the University of Tokyo (see **Fig. 1**). The test section had dimensions of 1.8 × 2.2 × 16.47 m^3 (height × width × length). The wind tunnel can provide adjustable inflow wind speed from 0.2 m/s to 20 m/s. Three vertical triangular spires and a large number of wooden cubes with dimensions of 3, 6 and 9 cm were placed upstream of the test section to generate and reproduce turbulence and the atmospheric boundary layer (ABL) profile.

Fig. 2 shows the profile of mean stream-wise velocity U and turbulence intensity I_u of approaching wind measured in the wind tunnel at the location of building center without building model. The velocity was measured by a constant-temperature hot wire anemometer, CT-HWA, with an X-wire probe (55P61, DANTEC). The mean wind velocity profile can be characterized by the power law:

$$\frac{U}{U_H} = (\frac{z}{H})^{\alpha} \quad (1)$$

where U_H is U at the building height H (In **Fig. 2**, U_H is 6.76 m/s), z is the height to the floor, and α is the power-law exponent (= 0.19).

2.2. Model and case description

The studied three-story model was a 1/30 reduce-scaled building with dimensions of 30 × 30 × 30 cm^3 ($H \times W \times W$). Each floor was 10 cm in height. For every ventilating case, only one floor was ventilated through one or two openings and the other two floors were sealed. **Fig. 3(a)** shows the building model of which the second floor was ventilated through two identical rectangular openings. As shown in **Fig. 3(b)**, width and height of each opening were both L_w (= 5 cm). The distance between the centerline of two openings was S, and the dimensionless opening separation was defined as $s' = S/W$.

The case arrangement considering different influencing factors on pumping ventilation is presented in **Table 1**. U_H was the same for all cases. Cases with no opening (s' = /) were included to clarify the effect of openings on the flow field around the building. s' = 0 refers to SS1. s' = 0.25, 0.50 and 0.75 refers to the three different opening separations for SS2 cases. In the following sections, a simplified form [s', floor] will be used to denote each case.

The formation of the pumping ventilation is due to the periodic vortex shedding induced by the instability of the two shear layer from the building sides. According to our former publications on pumping ventilation, the periodicity of pumping flow was clearly observed for a large range of *Re* from 1.1×10^5 to 8.75×10^7 considered in our former studies (Zhong et al., 2018, 2019a, 2019b, 2020). It is widely accepted that the mean flow characteristics will be similar if the Reynolds number is large enough (Townsend, 1956). The Reynolds number of the approaching flow based on the building height length scale was 120000, which was sufficiently larger than the recommended *Re* (> 4000) by Castro and Robins (1977) and also larger than the conservative *Re* (> 11000) suggested by Snyder (1981). Moreover, Tominaga and Stathopoulos (2018) confirmed that the difference was negligible between the measured velocities for *Re* = 5700 and that for *Re* = 57000 in wind tunnel experiments. Therefore, the flow field around the building in the present study could be considered self-similar with that in full-scale condition. Besides, the independence of *Re* inside the building of SSV can be expressed by *Re* based on the opening width scale, which was 20000 in this study. Kato et al. (2006) conducted wind tunnel experiments for SS1 and *Re* was 4700 based on the length scale of the opening width. Similarly, *Re* was between 5400 and 27000 in the experiments of Chu et al. (2011). In the most recent wind tunnel experiments of SS2 of a 1/20 scaled building (Albuquerque et al., 2020), *Re* of the reduced-scale building model was about 17500 based on the opening scale. Therefore, the flow field inside the building of SSV in this study was also supposed to be self-similar with that in full-scale condition.

2.3. Velocity measurements

The velocity measurements included the stream-wise instantaneous velocity at the right-side opening center point (also referred as u_w hereafter) and mean velocity distribution in the wake region of the building (U_x). Wind velocity was measured using a constant-temperature hot wire anemometer (CT-HWA) with a split-fiber probe (SFP), (55R55, DANTEC). The SFP can measure the adverse velocity for a wind direction. The

CT-HWA can measure the wind velocity from 0.02 to 300 m/s. The measuring accuracy depends on the calibration accuracy, which is typically around 0.5% and will not exceed 2%. The response time is short enough and can be negligible. The CT-HWA also enables accurate measurement of frequency up to 100 kHz and thus is sufficient for the measurement of pumping ventilation frequency.

A coordinate axis was defined and the coordinate origin is located at the center point of the bottom side of the rear surface (see **Fig. 3**). To measure the stream-wise velocity, the probe wire was placed horizontally, perpendicular to the stream-wise direction (see **Fig. 4**). Each measurement's period time was 120 s at a frequency of 1000 Hz, obtaining totally 1.2×10^5 sampling data. **To test the stability of the wind tunnel, normalized standard deviation of measured opening center velocity u_w for different measuring period time of case [s', floor] = [0.5, 2] is listed in Table 2. It is observed that the deviations between different sampling period times were lower than 1.00%, which could be negligible. Therefore it is believed that the velocity measurement was reliable and repeatable in the wind tunnel experiments.**

2.4. Frequency of pumping flow

We defined the pumping flow frequency as the frequency of the stream-wise wind velocity at the opening center point. From fast Fourier transform (FFT) of the velocity time history, we could obtain the dominant frequency *n* (Hz) corresponding to the peak of the power spectrum density (PSD) (see **Fig. 5**). Strouhal number was often used to denote the normalized vortex shedding frequency at the wake of a building (Lyn et al., 1995; Chen and Liu, 1999; Liu and Niu, 2016) and is nearly independent of *Re* between 10000 and 200000. In the present study, we also use this way to normalize the oscillation frequency of pumping flow of each floor and opening separation. The normalized pumping flow frequency St_w is defined as

$$St_w = nH/U_H \tag{2}$$

where *n* is the pumping flow frequency across the openings.

2.5. Ventilation rates

Measuring the airflow rate of a building model in the wind tunnel experiments is a difficult task. Instead, effective ventilation rates have been adopted by many researchers to quantify the ventilation effectiveness using tracer gas method (Albuquerque et al., 2020). In this study, ethylene (C_2H_4) was chosen as the tracer gas, mixed with nitrogen (N_2) to ensure security. The tracer gas was injected continuously at a total flow rate of 2 L/min (1.21 % C_2H_4) from 8 evenly spaced vertical rods (see Fig. 3(a), (c) and (d)). Each injection rod was half the height of the floor (H/6 = 5 cm). The concentrations were sampled using a fast flame ionization detector (FID) at the center point of the room, with a period of 120 s and at a frequency of 1000 Hz. **In the FID, negative ions are produced when hydrocarbons (C2H4) is burn. This ion is captured by the high voltage electrode, and the generated current is detected as an electric signal. The amount of generated ions is proportional to the number of carbon atoms in the burned hydrocarbon, so that the electrical signal and the hydrocarbon concentration in the sample gas are associated. H_2 and air are introduced into a burner frame as fuel gas to produce the above combustion reaction.** Each sampling period began 120 s after the tracer gas injection was started, to ensure a complete mixing of the tracer gas within the ventilated floor. FID can measure the concentration of tracer gas from 10 mV/ppm to 10 V/ppm and the response time is about several msec. **For concentration sampling of each case, measurements were conducted three times repeatedly and the arithmetic mean values of three repeated samplings were obtained.**

Purging flow rate (PFR) was adopted as the effective ventilation rate of the building model (Sandberg and Sjöberg, 1983). PFR quantifies the rate at which pollutants are removed from a homogeneously mixed region and thus can express the pollutant removal capability of a ventilation system. PFR can be obtained in the experiments as follows (Awbi, 2003):

$$PFR = \frac{Q}{\langle c \rangle} \quad (3)$$

where Q (L/min) is the injection rate of the tracer gas C_2H_4 and $\langle c \rangle$ represents the temporal spatial averaged concentration of C_2H_4 in the ventilated room. Since we assumed that the tracer gas in the ventilated room is completely mixed before sampling, the measured concentration by FID could be considered as the average equilibrium concentration in the room (Kato et al., 2006). $\langle c \rangle$ was finally calculated as the time-averaged value of the sampling period. The reference concentration c_0 was defined as

$$c_0 = \frac{Q}{H^2 U_H} \quad (4)$$

In order to remove the effect of room volume, air change per hour (*ACH*) was often used to evaluate the ventilation rate of building ventilation (Argiriou et al., 2002; Larsen and Heiselberg, 2008). Here we used ACH_{PFR} to define the air change rate (s^{-1}) of the ventilated floor based on *PFR* as follows:

$$ACH_{PFR} = \frac{PFR}{V_{room}} \quad (5)$$

where V_{room} (m^3) is the internal volume of the ventilated floor. ACH_{PFR} will also be referred as ventilation rate hereafter.

3. Results

3.1. Velocity distribution

To study the influence of openings on the velocity distribution in the wake region of the isolated building, three different cases, i.e. [s', floor] = [/, /] (no opening), [0, 2] (SS1) and [0.50, 2] (SS2), were considered. The stream-wise velocity (U_x) were measured and averaged at measuring points on three different vertical lines (x/H = 0.07, 0.125, 0.250, y/H = 0) and horizontal lines (x/H = 0.07, 0.125, 0.250, z/H = 0.5)，which were in the near wake region. In this region, the effect of the leeward façade openings on the flow characteristics could be the most significant. Each vertical/horizontal line had 8/9 measuring points respectively (see **Fig. 6**). **Fig. 6** reveals that the vertical and horizontal distributions of U_x for three cases were almost the same even for the measurement line that was closest to the leeward wall (x/H = 0.07). This is probably because that the openings were not very large openings and will not apparently affect the wake region flow characteristics. Therefore, the number of openings has negligible effects on the stream-wise velocity in the wake region of the building if the openings are not large enough.

3.2. Pumping flow frequency

The time histories of the stream-wise wind velocity u_w at the opening center of case [0, 2] (SS1) and [0.50, 2] (SS2) are shown in **Fig. 7**. u_w in SS2 showed more regular periodic oscillation than SS1 though periodic oscillation can be seen from both SS1 and SS2.

The oscillation frequency of pumping flow is represented by the St_w (**Eq. (2)**), normalized by U_H and H. The effect of opening separations (s') to St_w on different floors has been presented in **Fig. 8**. The range of St_w is generally between 0.12 and 0.54. For SS1, since the pumping flow does not exist, St_w of SS1 was not calculated. As illustrated in **Fig. 8**, St_w was nearly constant for the same floor and independent of the opening separation, i.e. about 0.12 on the first floor and about 0.16 on the second floor. The independence of pumping flow frequency from the opening separation was also reported by Zhong et al. (Zhong et al., 2019). For the third floor, St_w for the other two opening separations were also nearly the same and close to that on the second floor except the relatively larger St_w for $s' = 0.25$. It was probably because of the interference of another kind of vortex shedding (e.g. rooftop shedding or arch-type vortex shedding (Zhang et al., 2020), which suppressed the horizontal vortex shedding from the sidewalls and dominated the oscillating frequency at the rear openings. Due to the resistance of the ground to the periodic vortex shedding from the building, St_w was the lowest on the first floor for all s'. From the first to the upper floors, since the effect of ground becomes insignificant, the St_w got larger but no longer rised from the second to the third floor for $s' = 0.50$ and 0.75. Different floor corresponds to different frequency, which indicates that the pumping flow frequency is not always equals to the vortex shedding frequency considering different ventilating floors. St_w on the first floor is the closest to ($St = 0.12$) that reported by Liu & Niu (2016).

3.3. Ventilation rate

ACH_{PFR} of both SS1 and SS2 were calculated from **Eq. (5)**. **Fig. 9** shows the variation of ACH_{PFR} for different s' and floors. ACH_{PFR} on the first floor was the largest while that on the third floor was the smallest. As illustrated in **Fig. 8**, St_w at the openings on the first floor was the lowest. We can then deduce that the ventilation rate doesn't have a positive correlation with the pumping flow frequency. This conclusion was also supported in Zhong et al. (2020). On the whole, ACH_{PFR} is promoted when increasing the opening separation on the second and third floors, as reported in the former study (Zhong et al., 2019). However, there was a reduction of ACH_{PFR} from $s' = 0.50$ to 0.75 on the first floor, indicating that increasing the opening separation cannot necessarily promote the ventilation rate when the openings are on the first floor close to the ground surface. Nevertheless, the ventilation rate of SS2 was always larger than that of SS1 ($s' = 0$) with the same total opening area. ACH_{PFR} can be increased by up to about 123% compared with SS1 on the first floor ($s' = 0.50$), about 65% on the second floor and about 44% on the third floor.

3.4. Velocity and concentration fluctuations

Turbulent fluctuations could dominate the airflow field characteristics and air exchange of SSV for many wind directions (Furbringer and Maas, 1995; Chu et al., 2011). Velocity fluctuations across the opening thus played an important role in the ventilation rate. The center zone of a building is usually the most concerned occupied zone, thus the concentration fluctuation at the building center was measured to quantify the variation characteristics at that point. The time history of C_2H_4 concentration for case [0.5, 2] is shown in Fig. 10(a). It can be observed that the concentration shows nearly periodic variation with time.

The standard deviation (SD) of the stream-wise wind velocity at the opening center SD_u was normalized by U_H ($\sigma_u = SD_u/U_H$) and the SD of C_2H_4 concentration SD_c was normalized by c_0 ($\sigma_c = SD_c/c_0$).

The correlation between σ_u and s' differed a lot from that between ACH_{PFR} and s'. σ_u reached its maximum values at lower opening separations, i.e. s' = 0.25 or 0.50, and relatively lower σ_u occurred at the largest opening separation (s' = 0.75) and SS1 (s' = 0). σ_u on the first and third floors were the largest and smallest, respectively (see **Fig. 10 (b)**).

The correlation between the concentration fluctuation and the opening separation on different floors is presented in **Fig. 10 (c).** σ_c on the first floor was the most sensitive to s' and decreased rapidly with the increase of s' while σ_c on the second and third floors were less affected by s'. For SS2, the concentration fluctuation of the second floor was the largest while which floor had the lowest σ_c depended on the opening separation and could not be simply concluded. However, the ventilation rate on the third floor was the lowest. It can be found that the ventilation rate and σ_c were not positively correlated for pumping ventilation.

As σ_c could not express the relative instability of concentration for different cases, concentration fluctuation intensity was adopted, normalizing the standard deviation of concentration by mean concentration (Lin et al., 2020). It expresses the relative instability of the concentration and is defined as $I_c = \sigma_c / \langle c \rangle$.

The concentration fluctuation intensity at different opening separations is shown in **Fig. 11**. For SS2 ($s' \geq 0.25$), the instability of concentration was strengthened when opening separation s' became larger on the second and third floors. However, it became stable when s' increased on the first floor, in compliance with the results that the ventilation rate also decreased at larger opening separation on the first floor.

I_c on the third floor was the most stable among the three different floors. We can also find from **Fig. 10 (b)** that σ_u on the third floor was the lowest, indicating that the pumping flow on the third floor, i.e. the top floor, was the most insignificant. This result also consists with that in Sec. 3.3, reporting that the lowest ventilation rate ACH_{PFR} occurred on the third floor. The insignificance of pumping flow on the third floor was probably due to the fact that pumping flow could be easily disturbed by the roof shedding flows.

Fig. 12 presents the probability density function (PDF) of concentration for different opening separations s', and ventilated floors. The horizontal coordinate value denotes the degree of deviation from average concentration. The positive deviation was always larger than the negative deviation. The positive deviation for $s' = 0.25$ was the largest among four s' (**Fig. 12 (a)**). Both the negative and the positive deviation of the second floor were the largest among three floors (**Fig. 12 (b)**).

4. Discussion

This research investigated the pumping ventilation on different floors, which was not considered in former publications. Literature review indicated that former ones only discussed about the pumping flow on the middle floor or through openings located at the middle height of the building. The pumping ventilation was much “purer” and less affected by the ground or the rooftop shedding flows on the middle floors. However, as investigated in this paper, St_w on the first floor and ACH_{PFR} on the third floor sometimes showed different correlation with the opening separations. Hence, the existing rules concluded by past investigations of pumping ventilation may not be applicable for all floors of a multi-story building, especially on the bottom and the top floors.

Certainly, present study on pumping ventilation was still limited in the ideal and theoretical level. As pumping ventilation is mostly a horizontal wind behavior, the vertical mutual influence may not be significant. Nevertheless, it would certainly be better if the openings on every floor are opened to consider the mutual influence between openings on different floors, which will be included in our further studies. In addition, the contribution of the velocity fluctuations to the ventilation rate of pumping ventilation still need to be quantified with the help of CFD simulation. The present experimental study on pumping ventilation is still an early stage of the pumping ventilation study in the real buildings in urban areas.

5. Conclusions

This study presented wind tunnel experiments on the pumping ventilation of an isolated three-story building model. Opening separation and ventilated floor represented main influencing factors. The wind velocity was measured by CT-HWA and the ventilation rate was represented by ACH_{PFR} and obtained using tracer-gas method. Main conclusions were summarized as follows,

(1) St_w was independent of the opening separation on the first and second floor except an extraordinary large St_w on the third floor probably because of the disturbance of the rooftop shedding frequency. St on the first floor became the lowest due to the effect of the ground to the vortex shedding.

(2) The ventilation rate (ACH_{PFR}) of SS2 was always higher than that of SS1 with the same total opening area. The ventilation rate could be promoted by increasing the opening separation while on the first floor the ventilation rate may start to decrease for large opening separation. The ventilation rate on the first floor was the highest while that on the third floor became the smallest. ACH_{PFR} could be increased up to about 123% comparing with that of SS1 on the first floor, about 65% on the second floor and about 44% on the third floor.

(3) Neither the opening center wind velocity fluctuation nor the indoor concentration fluctuation was positively correlated with the ventilation rate of pumping ventilation. The response of velocity and concentration fluctuation to the opening separation and ventilated floor were not consistent.

(4) The conclusion of this study can be applied to generic building configurations and may be no longer applicable for buildings with other different shapes, structures or for buildings with very large openings. The pumping ventilation for more building configurations still requires further investigation in the following studies.

Acknowledgements

This research was financially supported by the ***Natural Science Foundation of China*** (NSFC Grant No. 51778504; Grant No. U1867221), ***Science and Technology Innovation Leader of Hunan Province*** (Grant No. 2020RC4032, Hunan University of Technology), ***Fundamental Research Funds for the Central Universities*** (Grant No. 2042020kf0203, Wuhan University), and ***National Key Research and Development Program of the Ministry of Science and Technology of China*** (Grant No. 2018YFC0705201, Grant No. 2018YFB0904200).

References

B. Chenari, J. Carrilho, M. Silva. Towards sustainable, energy-efficient and healthy ventilation strategies in buildings: A review, ***Renewable and Sustainable Energy Reviews***, 59 (2016) 1426-1447.

C. Allocca, Q.Y. Chen, L.R. Glicksman. Design analysis of single–sided natural ventilation, ***Energy and Buildings***, 35 (2003) 785-795.

J.P. Cockroft, P. Robertson. Ventilation of an enclosure through a single opening, ***Building and Environment*** 11 (1976) 29-35.

P.R. Warren. Ventilation through openings on one wall only. In International Centre for Heat and Mass Transfer Conference: Energy Conservation in Heating, Cooling and Ventilating Buildings; Hoogendorn, C.J., Afgar, N.H., Eds.; Hemisphere Publishing Corporation: Dubrovnik, Yugoslavia, 1977; Volume 1, pp. 189–209.

Z.T. Ai, C.M. Mak. Determination of single-sided ventilation rates in multistory buildings: Evaluation of methods, ***Energy and Buildings*** 69 (2014) 292-300.

E. Dascalaki, M. Santamouris, A. Argiriou et al. Predicting single sided natural ventilation rates in buildings, ***Solar Energy*** 55 (1995) 327-341.

Y. Jiang, Q. Chen. Buoyancy-driven single-sided natural ventilation in buildings with large openings, ***International Journal of Heat and Mass Transfer*** 46 (2003) 973-988.

Y. Jiang, D. Alexander, H. Jenkins, R. Arthur, Q. Chen. Natural ventilation in buildings: measurement in a wind tunnel and numerical simulation with large-eddy simulation, ***Journal of Wind Engineering and Industrial Aerodynamics*** 91 (2003) 331-353.

W.De Gids, H. Phaff. Ventilation rates and energy consumption due to open windows, ***Air Infiltration Review*** 4 (1982) 4-5.

C.R. Chu, Y.H. Chiu, Y.T. Tsai, S.-L. Wu. Wind-driven natural ventilation for buildings with two openings on the same external wall, ***Energy and Buildings*** 108 (2015) 365-372.

J. Cermak. Wind tunnel studies of buildings and structures, ***American Society of civil engineers***, 1999.

M.M. Eftekhari, L.D. Marjanovic, D.J. Pinnock. Air flow distribution in and around a single-sided naturally ventilated room, ***Building and Environment*** 38 (2003) 389-397.

S. Kato, R. Kono, T. Hasama, R. Ooka, T. Takahashi. A wind tunnel experimental analysis of the ventilation characteristics of a room with single-sided opening in uniform flow, ***International Journal of Ventilation*** 5 (2006) 171-178.

T. Yamanaka, H. Kotani, K. Iwamoto, M. Kato. Natural, wind-forced ventilation caused by turbulence in a room with a single opening, ***International Journal of Ventilation*** 5 (2006) 179-187.

T.S. Larsen, P. Heiselberg. Single-sided natural ventilation driven by wind pressure and temperature difference, ***Energy and Buildings*** 40 (2008) 1031-1040.

Z. Bu, S Kato. Wind-induced ventilation performances and airflow characteristics in an areaway-attached basement with a single-sided opening, ***Building and Environment*** 46 (2011) 911-921.

C.R. Chu, R.-H. Chen, J.-W. Chen. A laboratory experiment of shear-induced natural ventilation, ***Energy and Buildings*** 43 (2011) 2631–2637.

R. Freire, M. Abadie, N. Mendes. On the improvement of natural ventilation models, ***Energy and Buildings*** 62 (2013) 222-229.

T. Larsen, C. Plesner, V. Leprince, F. Carrié, A. Bejder. Calculation methods for single-sided natural ventilation: Now and ahead, ***Energy and Buildings*** 177 (2018) 279-289.

J. Lu, J. Gu, K. Li et al. COVID-19 Outbreak Associated with Air Conditioning in Restaurant, Guangzhou, China, 2020, ***Emerging Infectious Diseases*** 26 (2020) 1628-1631.

N.C. Daish, G. Carrilho da Graça, P.F. Linden, D. Banks. Impact of aperture separation on wind-driven single-sided natural ventilation, ***Building and Environment*** 108 (2016) 122-134.

G. Carrilho da Graça, P. Linden. Ten questions about natural ventilation of non-domestic buildings, ***Building and Environment*** 107 (2016) 263-273.

H. Zhong, D.D. Zhang, D. Liu, F.Y. Zhao, Y.G. Li, H.Q. Wang. Two dimensional numerical simulation of wind driven ventilation across a building enclosure with two free apertures on the rear side: Vortex shedding and "pumping flow mechanism", ***Journal of Wind Engineering and Industrial Aerodynamics*** 179 (2018) 449–462.

A.A.R. Townsend. The Structure of Turbulent Shear Flow. Cambridge university press, 1956.

I.P. Castro, A.G. Robins. The flow around a surface-mounted cube in uniform and turbulent streams. ***Journal of Fluid Mechanics*** 79 (1977) 307-335.

W.H. Snyder. *Guideline for Fluid Modeling of Atmospheric Diffusion*, 1981.

Y. Tominaga, T. Stathopoulos. CFD simulations of near-field pollutant dispersion with different plume buoyancies, ***Building and Environment*** 131 (2018) 128-139.

D. Albuquerque, M. Sandberg, P. Linden, G. Carrilho da Graça. Experimental and numerical investigation of pumping ventilation on the leeward side of a cubic building, ***Building and Environment*** 179 (2020) 106897.

A.A. Argiriou, C.A. Balaras, S.P. Lykoudis. Single-sided ventilation of buildings through shaded large openings, ***Energy*** 27 (2002) 93-115.

B. Zhang, R. Ooka, H. Kikumoto. Analysis of turbulent structures around a rectangular prism building model using spectral proper orthogonal decomposition, ***Journal of Wind Engineering & Industrial Aerodynamics*** 206 (2020) 104213.

H. Zhong, D. Zhang, Y. Liu, D. Liu, F. Zhao, Y. Li, H. Wang. Wind driven “pumping” fluid flow and turbulent mean oscillation across high-rise building enclosures with multiple naturally ventilated apertures, ***Sustainable Cities and Society*** 50 (2019) 101619.

H. Zhong, Y. Jing, Y. Liu, F. Zhao, D. Liu, Y. Li. CFD simulation of “pumping” flow mechanism of an urban building affected by an upstream building in high Reynolds flows, ***Energy and Buildings*** 202 (2019) 109330.

H. Zhong, Y. Jing, Y. Sun, H. Kikumoto, F. Zhao, Y. Li. Wind-driven pumping flow ventilation of highrise buildings: Effects of upstream building arrangements and opening area ratios, ***Science of the Total Environment*** 722 (2020) 137924.

Chao Lin, Ryozo Ooka, Hideki Kikumoto, Taiki Sato, Maiko Arai. Wind tunnel experiment on high-buoyancy gas dispersion around isolated cubic building, ***Journal of Wind Engineering & Industrial Aerodynamics*** 202 (2020) 104226.

D.A. Lyn, S. Einav, W. Rodi, J.H. Park, A laser-Doppler velocimetry study of ensemble-averaged characteristics of the turbulent near wake of a square cylinder, ***Journal of Fluid Mechanics*** 304 (1995) 285-319.

J.M. Chen, C.H. Liu, Vortex shedding and surface pressures on a square cylinder at incidence to a uniform air stream, ***International Journal of Heat and Fluid Flow*** 20 (1999) 592-597.

J. Liu, J. Niu. CFD simulation of the wind environment around an isolated high-rise building: An evaluation of SRANS, LES and DES models, ***Building and Environment*** 96 (2016) 91-106.

M. Sandberg, M. Sjöberg. The use of moment for assessing air quality in ventilated rooms, ***Building and Environment*** 18 (1983) 181–97.

H. Awbi. Ventilation of buildings. Taylor & Francis, 2003.

J. Furbringer, J. Maas. Suitable algorithms for calculating air renewal rate by pulsating air flow through a single large opening, ***Building and Environment*** 30 (1995) 493-503.

A. Okajima. Strouhal Numbers of Rectangular Cylinders, ***Journal of Fluid Mechanics*** 123 (1982) 379-398.

T. Nakagawa. Vortex shedding behind a square cylinder in transonic flows, ***Journal of Fluid Mechanics*** 178 (1987) 303-323.

C.W. Knisely. Strouhal numbers of rectangular cylinders at incidence: a review and new data, ***Journal of Fluid and Structures*** 4 (1990) 371–393.

H. Nakaguchi, K. Hashimoto, S. Muto. An experimental study on aerodynamic drag of rectangular cylinders, ***The Journal of the Japan Society of Aeronautical Engineering*** 16 (1968) 1-5.

Y. Tominaga, A. Mochida, S. Murakami, S. Sawaki. Comparison of various revised k-ε models and LES applied to flow around a high-rise building model with 1:1:2 shape placed within the surface boundary layer, ***Journal of Wind Engineering and Industrial Aerodynamics*** 96 (2008) 389-411.

J. Liu, J. Niu. CFD simulation of the wind environment around an isolated high-rise building: an evaluation of SRANS, LES and DES models, ***Building and Environment*** 96 (2016) 91-106.

F. Wang, K.M. Lam, G.B. Zu, L. Cheng. Coherent structures and wind force generation of square-section building model, ***Journal of Wind Engineering and Industrial Aerodynamics*** 188 (2019) 175-193.

Y. Hui, K. Yuan, Z. Chen, Q. Yang. Characteristics of aerodynamic forces on high-rise buildings with various façade appurtenances, Journal of Wind Engineering and Industrial Aerodynamics 191 (2019) 76-90.

S. Huang, Q.S. Li, S. Xu. Numerical evaluation of wind effects on a tall steel building by CFD, ***Journal of Constructional Steel Research*** 63 (2007) 612-627.

J. Liu, J. Niu, C.M. Mak, Q. Xia. Detached eddy simulation of pedestrian-level wind and gust around an elevated building, ***Building and Environment*** 125 (2017) 168-179.

Figure 01

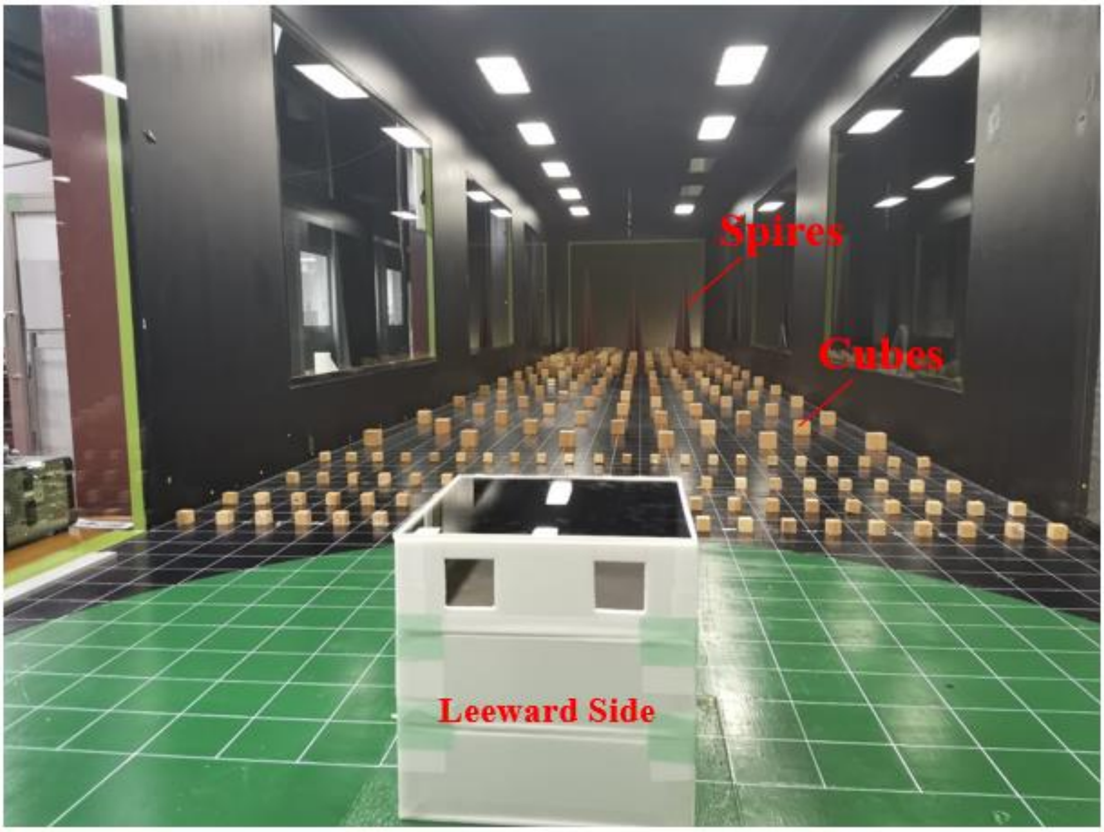

Fig. 1. The boundary layer wind tunnel.

Figure 02

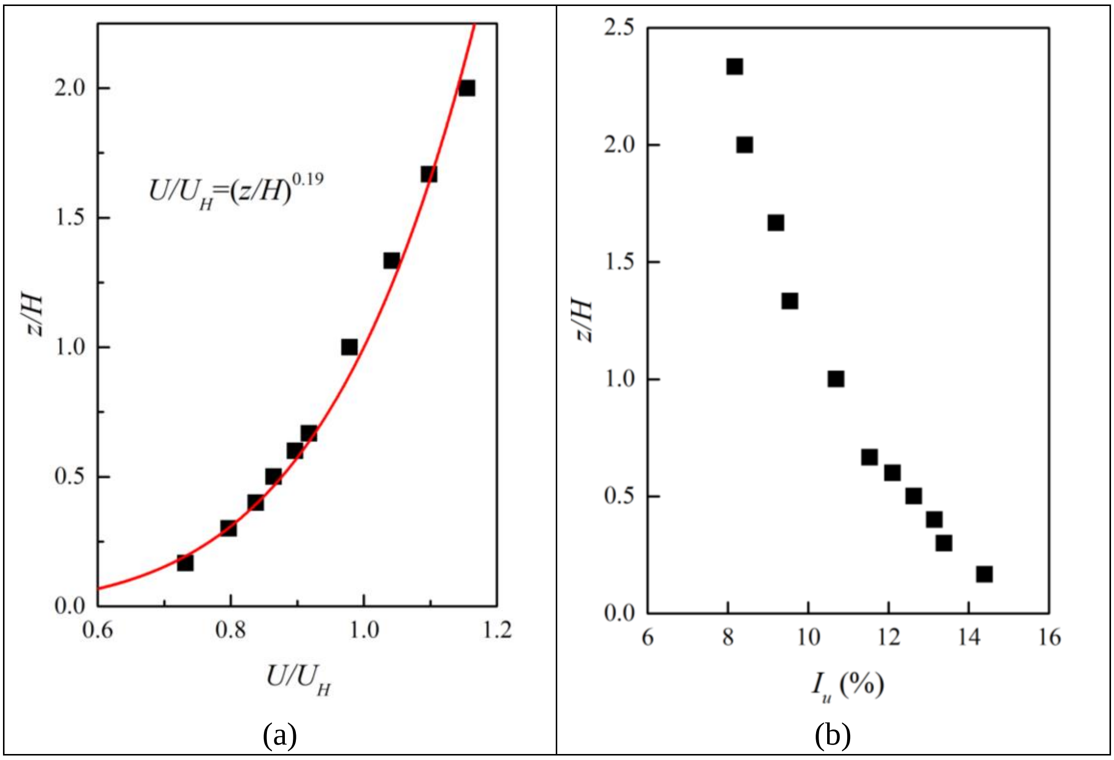

Fig. 2. Inflow boundary condition of the wind tunnel: (a) mean stream-wise wind velocity; (b) turbulence intensity.

Figure 03

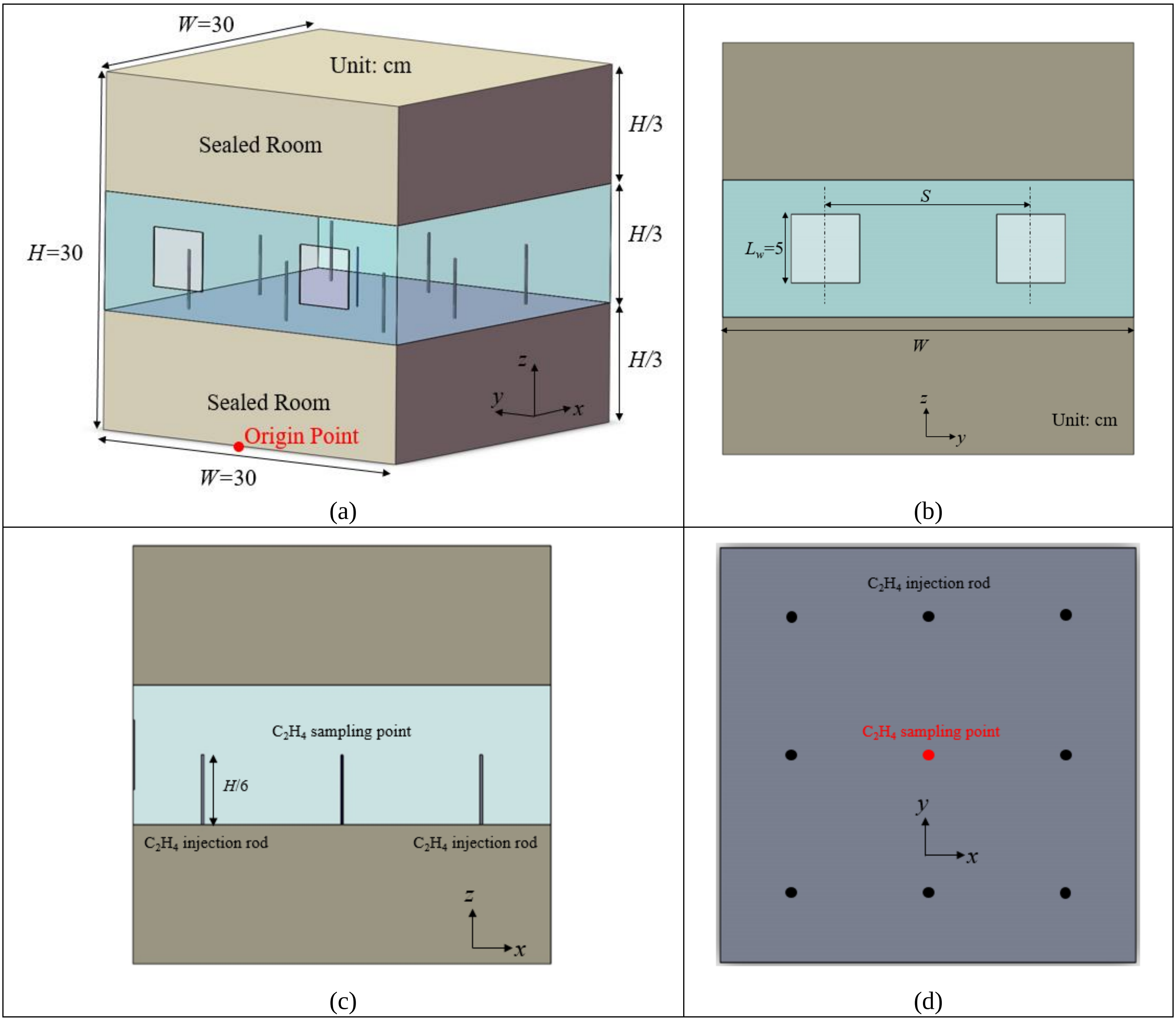

Fig. 3. The building model used in the wind tunnel experiments: (a) dimensions of the building model; (b) opening configurations; (c) side view of the model; (d) top view of the ventilated floor.

Figure 04

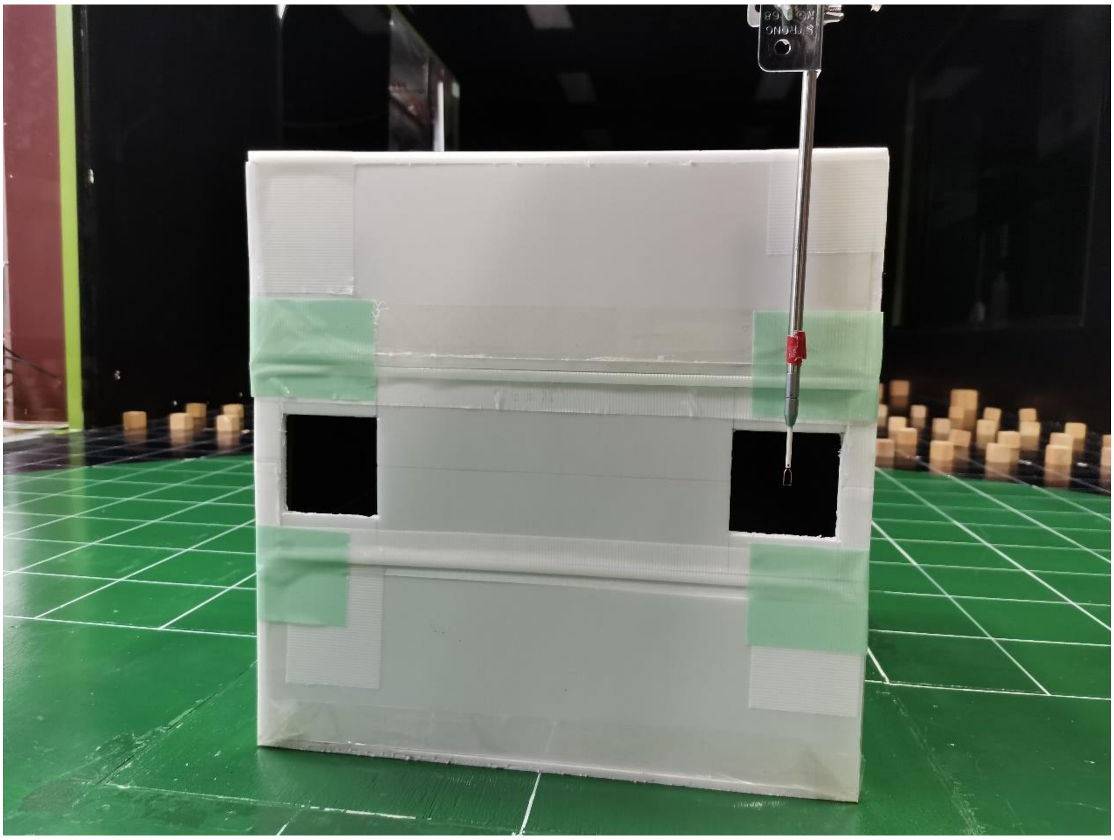

Fig. 4. SFP placement in the stream-wise wind velocity measurements.

Figure 05

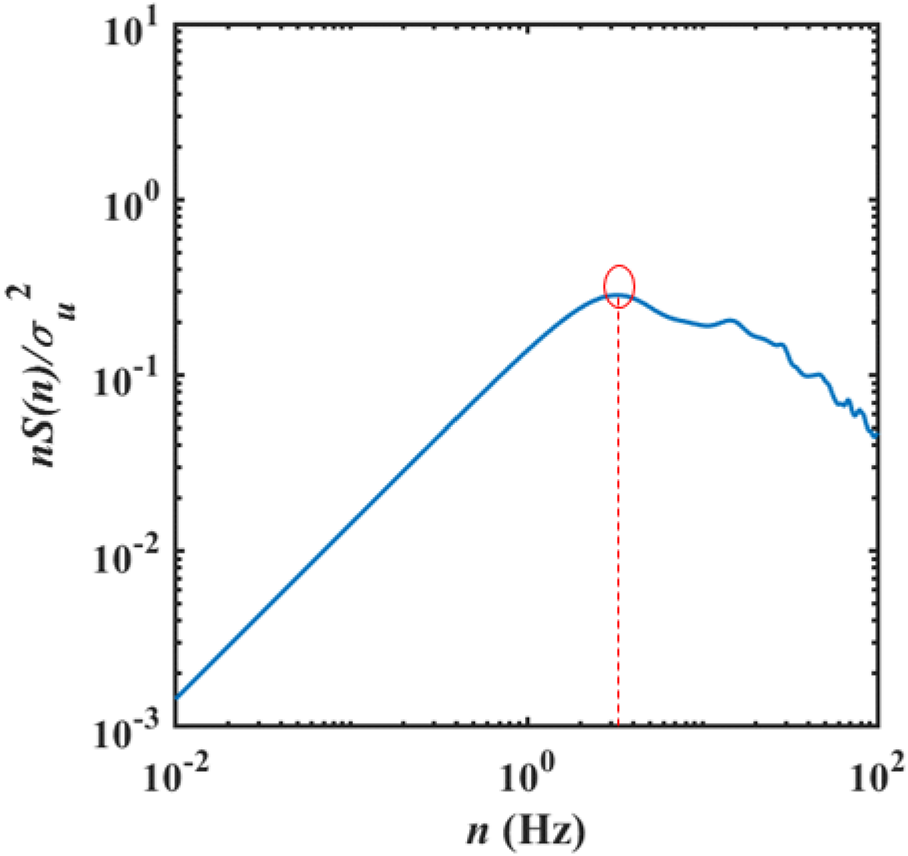

Fig. 5. Power spectrum density (PSD) for obtaining the “pumping” flow frequency. The circle denotes the dominant frequency.

Figure 06

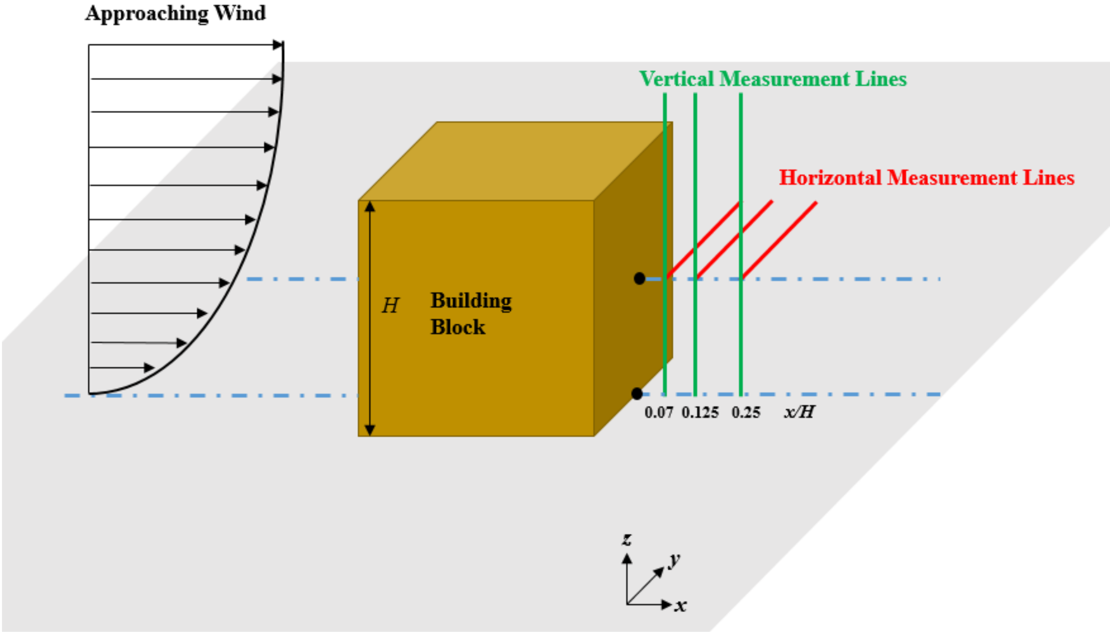

(a) 3D layout of velocity measurement lines

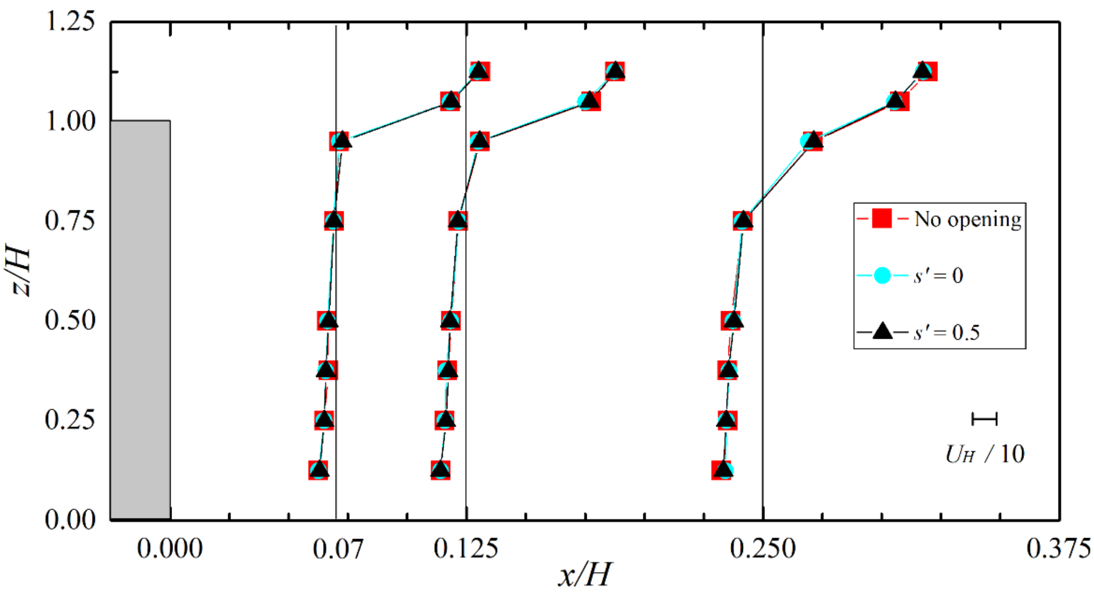

(b) Velocity distributions in vertical lines

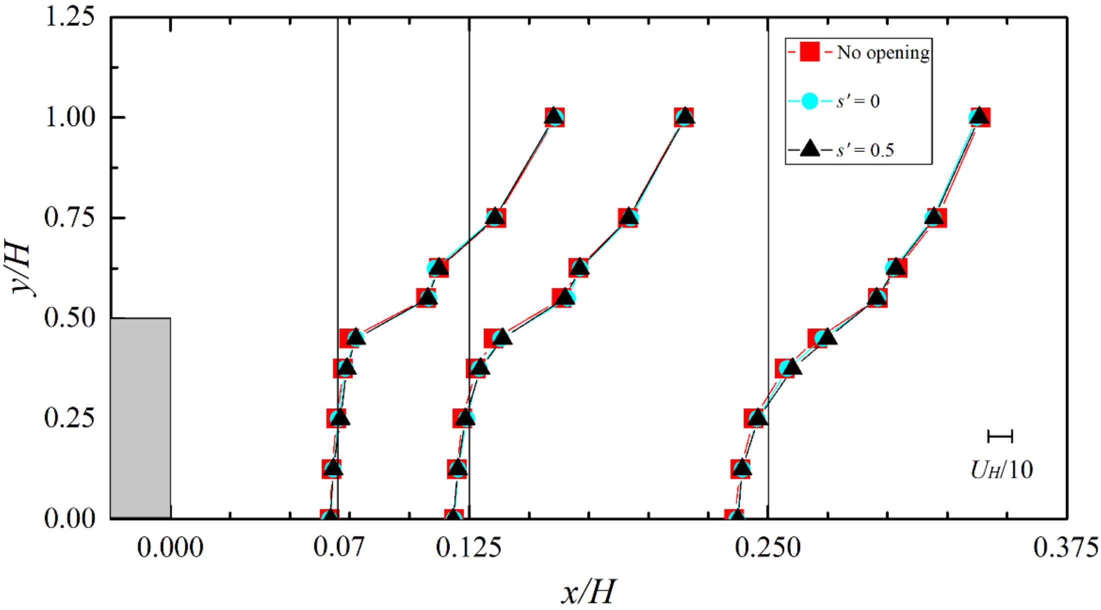

(c) Velocity distributions in horizontal lines

Fig. 6. (a) 3D layout of velocity measurement lines and the profiles of mean stream-wise velocity (U_x) on the (a) vertical and (b) horizontal sections for cases [/, /] (no opening), [0, 2] (SS1) and [0.50, 2] (SS2).

Figure 07

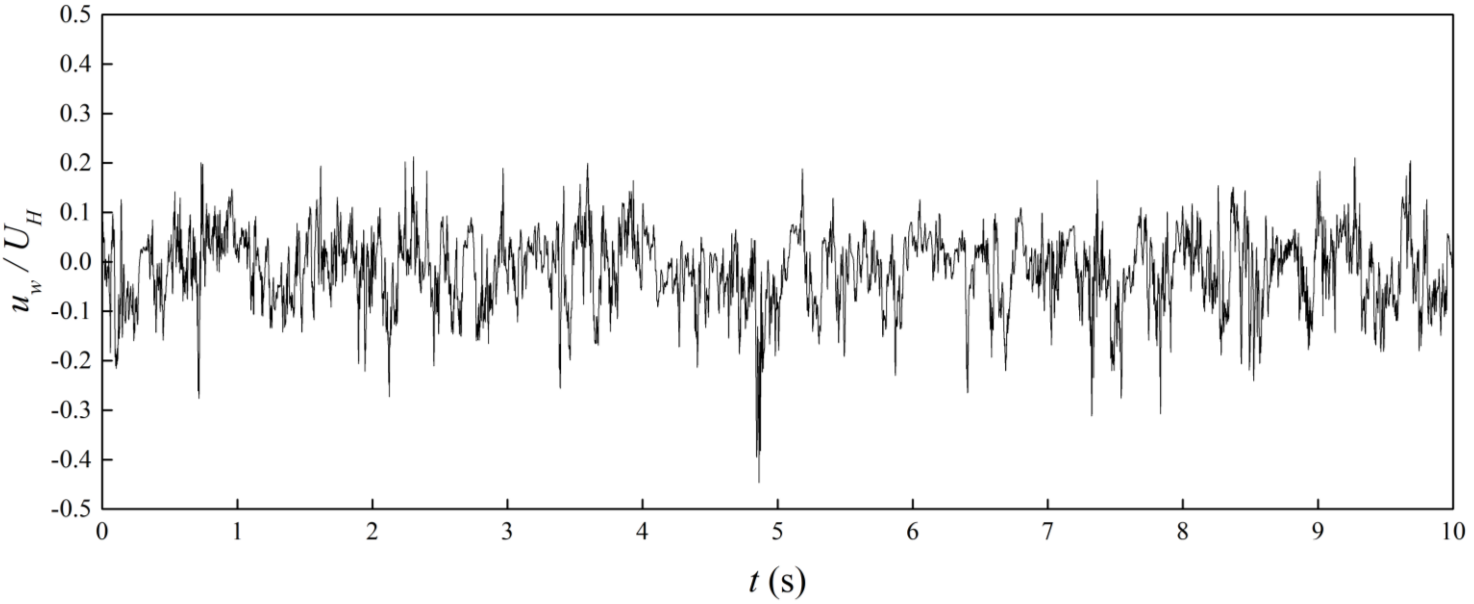

(a)

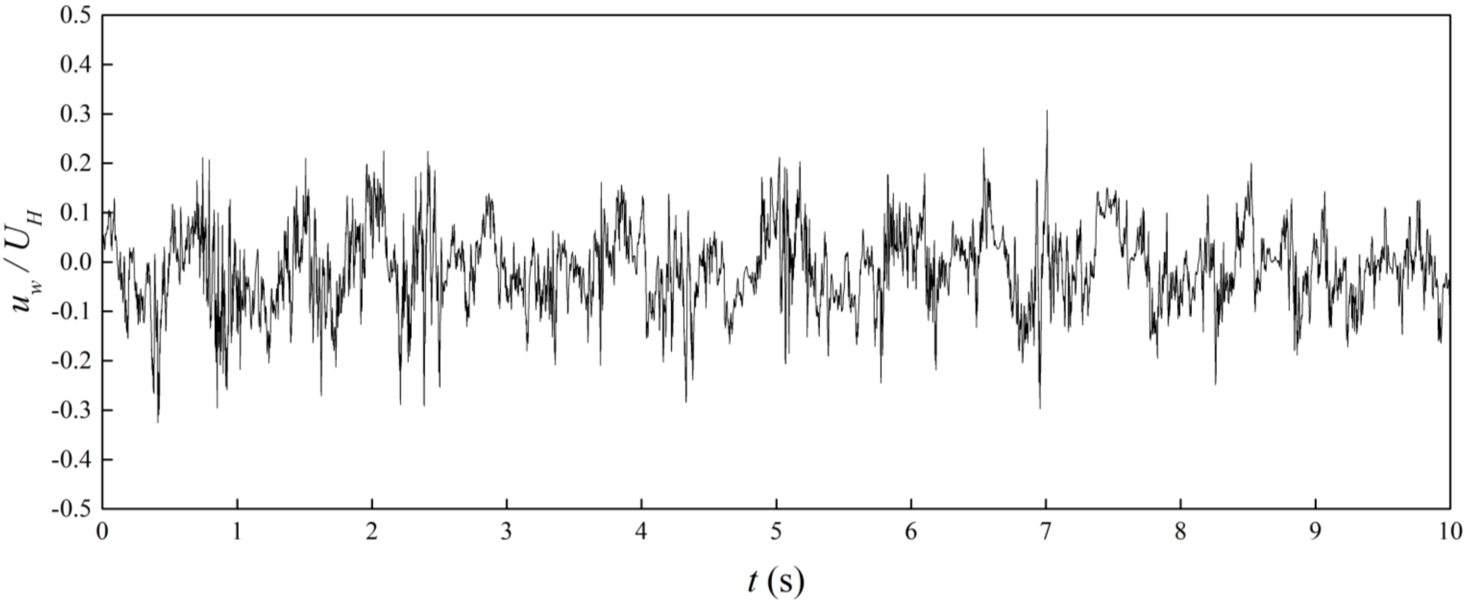

(b)

Fig. 7. The time history of the instantaneous stream-wise wind velocity u_w at the opening center of (a) case [0, 2] (SS1) and (b) case [0.50, 2] (SS2) in 10 s.

Figure 08

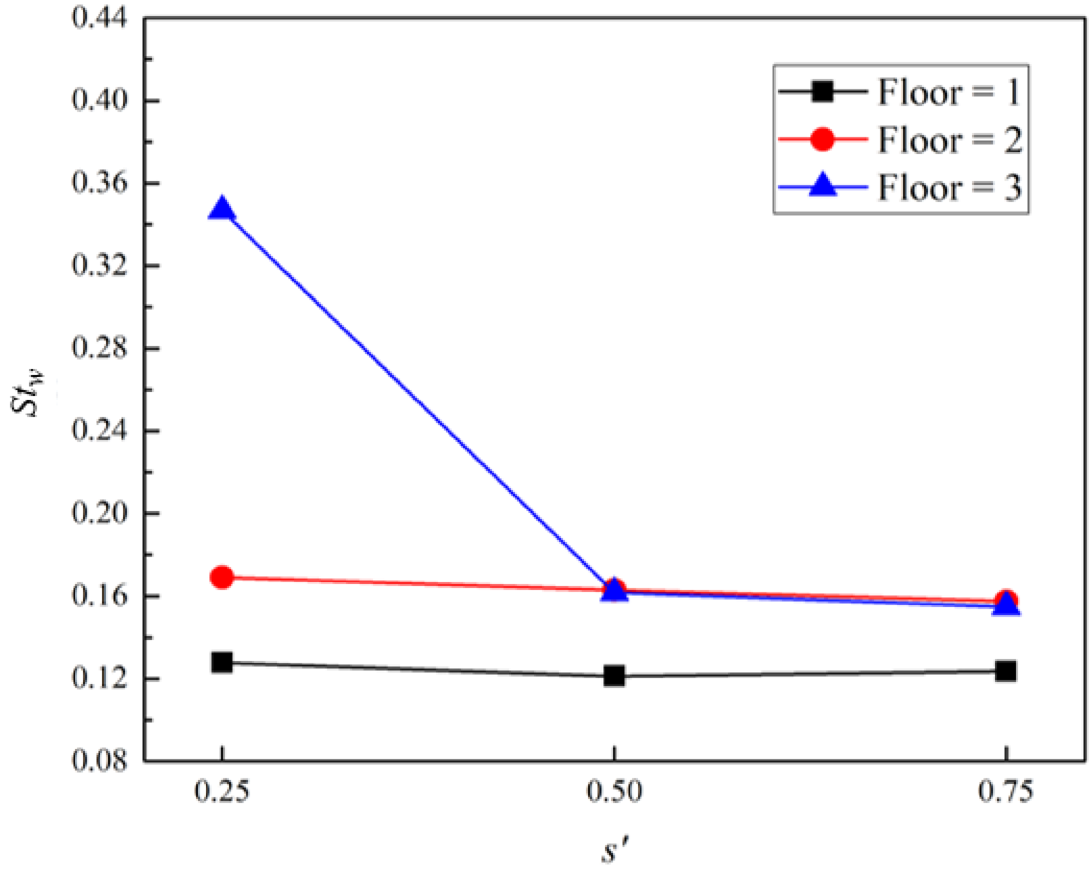

Fig. 8. Variations of St_w with different s' and ventilating floor.

Figure 09

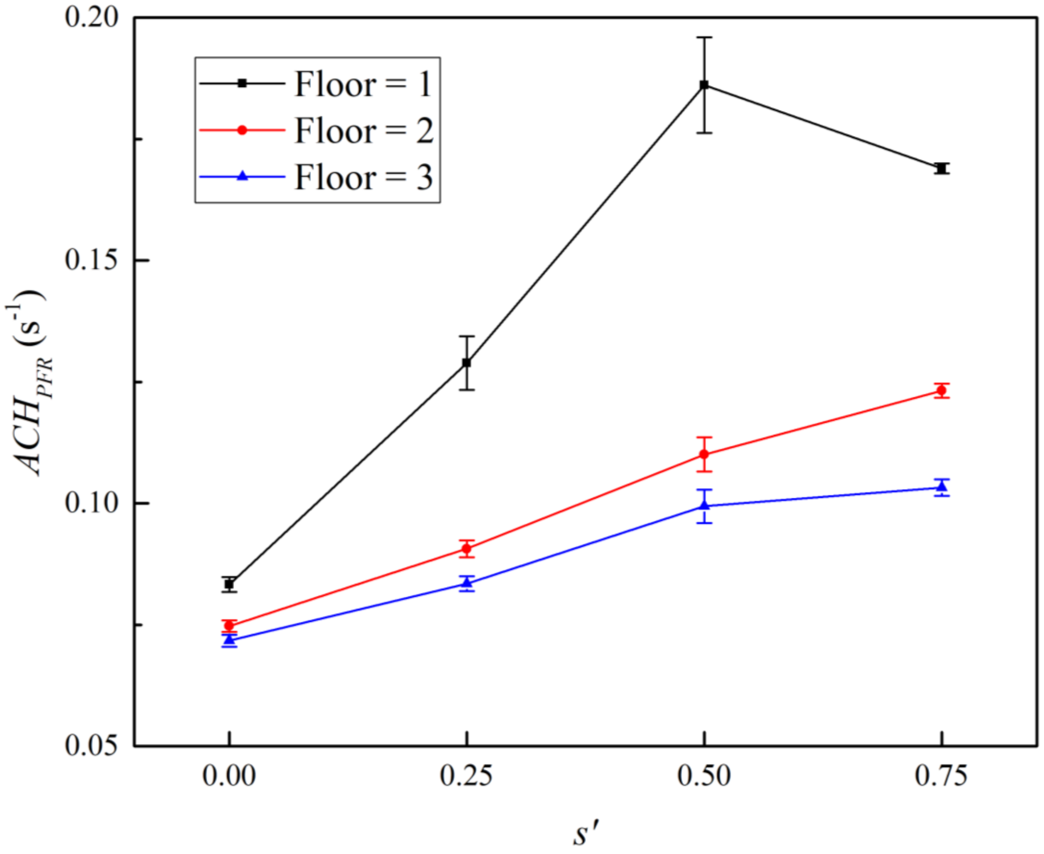

Fig. 9. Variations of ACH_{PFR} with different s' and ventilating floor.

Figure 10

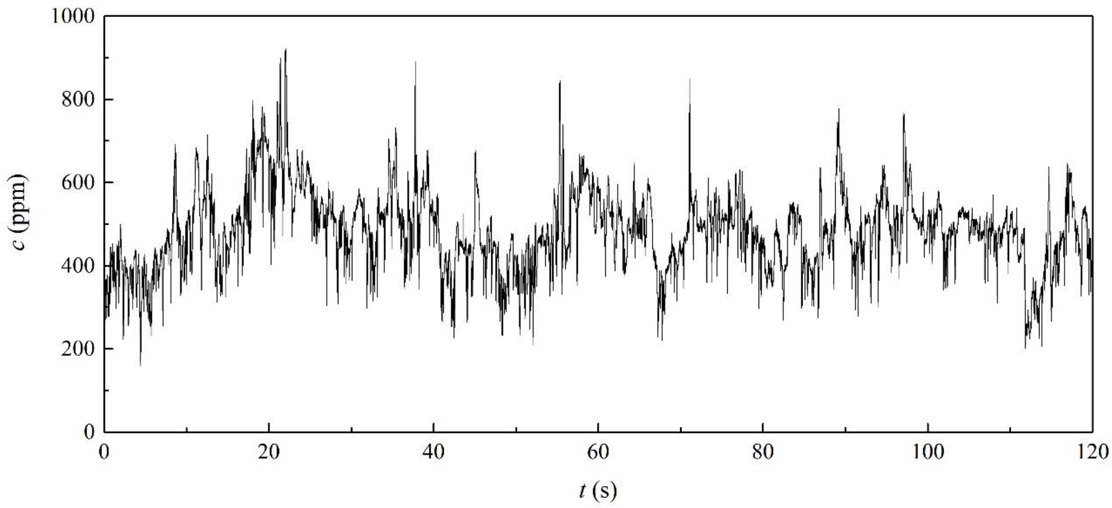

(a)

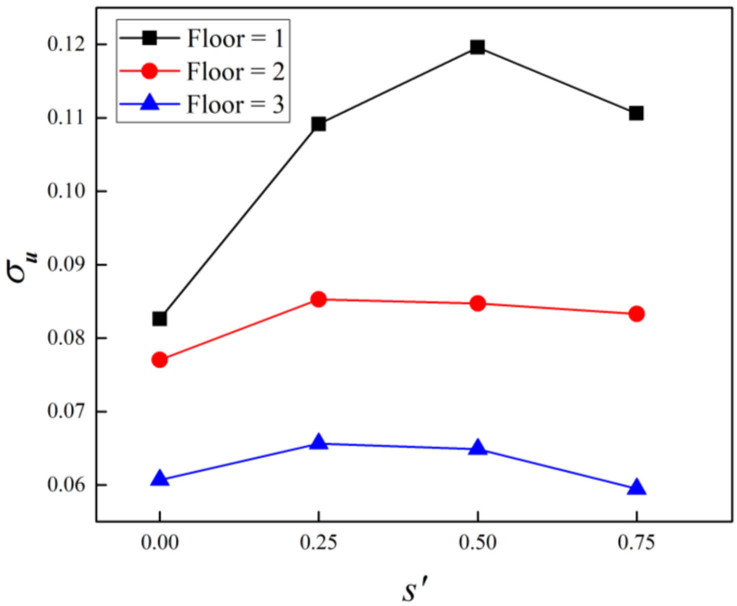

(b)

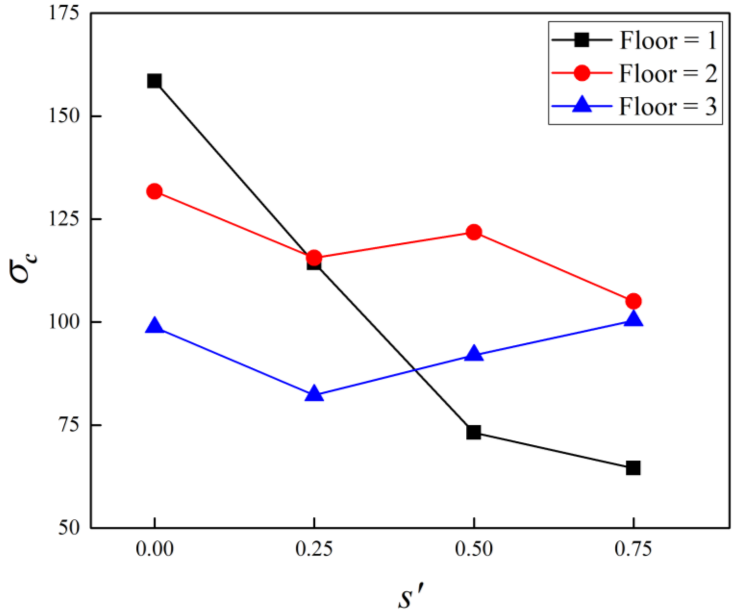

(c)

Fig. 10. (a) Time history of C_2H_4 concentration for case [0.5, 2] and Variations of (b) σ_u and (c) σ_c with different s' and ventilating floor.

Figure 11

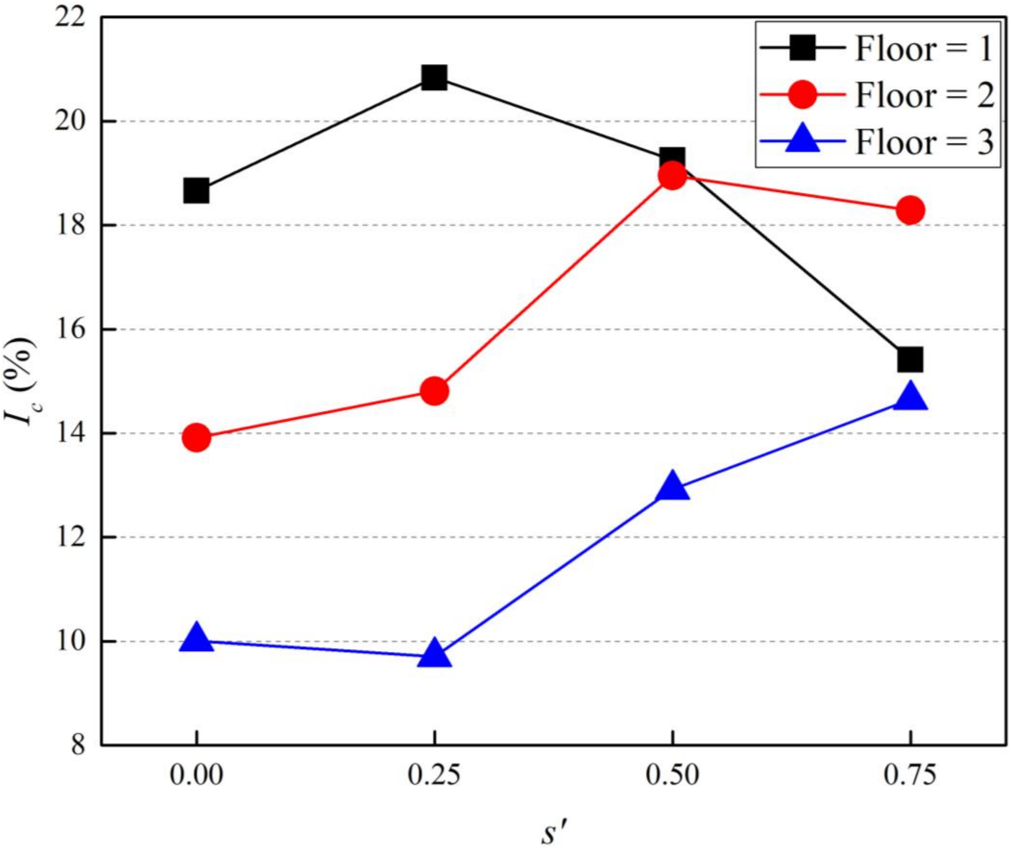

Fig. 11. Variations of I_c with different s' on different floors.

Figure 12

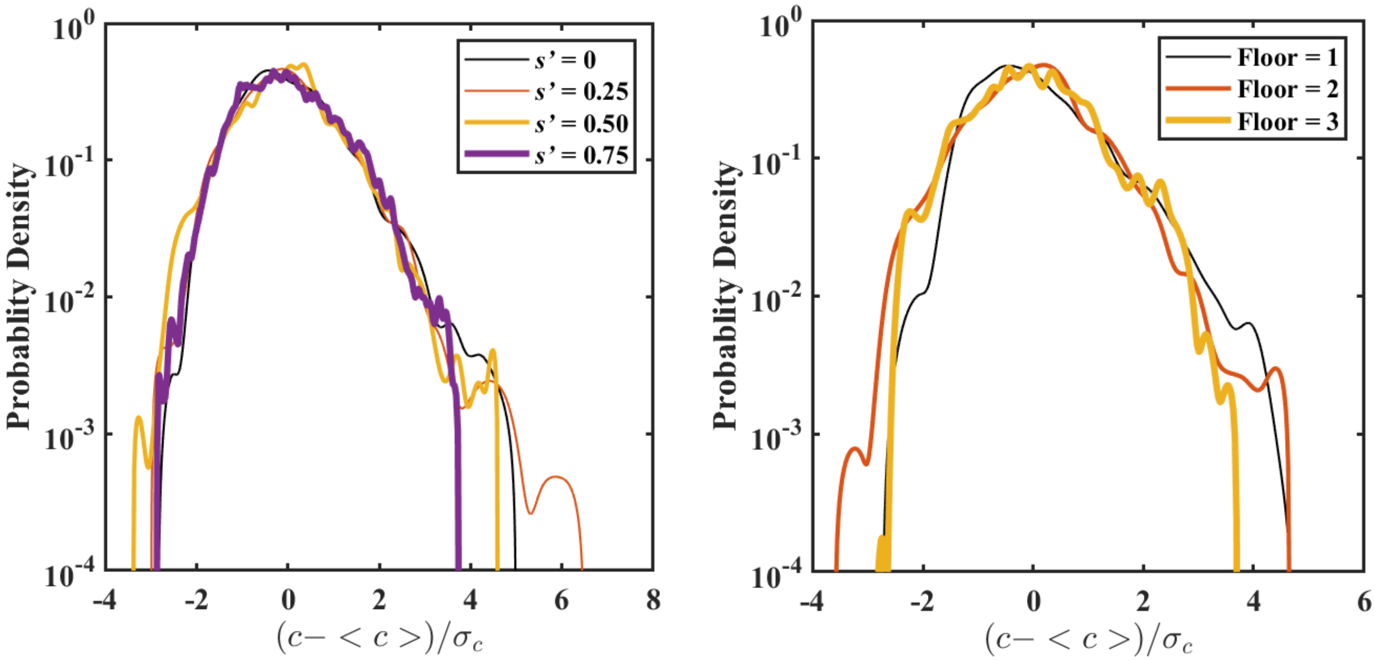

(a) (b)

Fig. 12. Probability density function of C_2H_4 concentration: (a) effect of different s'; (b) effect of ventilating floor.

Table 01

Table 1. Case arrangements

Opening Strategy	s'	Floor	Total Case Numbers
No Opening	/	/	1
SS1	0	1, 2, 3	3
SS2	0.25	1, 2, 3	3
SS2	0.50	1, 2, 3	3
SS2	0.75	1, 2, 3	3

Floor: the ventilating floor with openings;
"/": cases without opening;
$s' = 0$: single opening (SS1).

Table 02

Table 2. Normalized standard deviation of measured u_w for different measuring period time of case [0.5, 2]

Sampling Time (s)	SD_w/U_H ($\times 10^{-3}$)	Deviation from whole period (%)
60	75.661	0.64
90	75.937	1.00
120	75.182	---

Nomenclature

H	Building height (m)
U	Incident stream-wise mean wind velocity (m/s)
U_H	Mean approaching stream-wise velocity at building height (m/s)
z	Height to the floor (m)
α	Power-law exponent
W	Width of the building (cm)
L_w	Width and height of each opening (cm)
S	Distance between the centerline of two openings (cm)
s'	Dimensionless opening separation
n	Frequency (Hz)
St	Strouhal number
Q	Injection rate of the tracer gas C_2H_4, (L/min)
c_0	Reference concentration of C_2H_4 (ppm)
c	Instantaneous concentration of C_2H_4 (ppm)
$\langle c \rangle$	Temporal spatial averaged concentration (ppm)
PFR	Purging flow rate (m^3/s)
U_x	Mean stream-wise wind velocity (m/s)
V_{room}	The internal volume of the ventilated floor (m^3)
ACH_{PFR}	Air change rate of the ventilated floor base on *PFR* (s^{-1})
u_w	Instantaneous stream-wise velocity at the window center (m/s)
St_w	Normalized pumping flow frequency
SD_u	Standard deviation of the stream-wise wind velocity at the opening center (m/s)
SD_c	Standard deviation of C_2H_4 concentration (ppm)
σ_u	Normalized standard deviation of the stream-wise wind velocity at the window center
σ_c	Normalized standard deviation of C_2H_4 concentration
I_c	Concentration fluctuation intensity of C_2H_4 (%)